NASA TECHNICAL NOTE

NASA TN D-4546

C.1

NASA TN D-4546

EXPERIMENTAL INVESTIGATION OF REACTOR-LOOP TRANSIENTS DURING STARTUP OF A SIMULATED SNAP-8 SYSTEM

by Pierre A. Thollot, Henry B. Block, and Kent S. Jefferies

Lewis Research Center
Cleveland, Ohio

NATIONAL AERONAUTICS AND SPACE ADMINISTRATION • WASHINGTON, D. C. • MAY 1968

NASA TN D-4546

EXPERIMENTAL INVESTIGATION OF REACTOR-LOOP TRANSIENTS DURING STARTUP OF A SIMULATED SNAP-8 SYSTEM

By Pierre A. Thollot, Henry B. Block, and Kent S. Jefferies

Lewis Research Center
Cleveland, Ohio

NATIONAL AERONAUTICS AND SPACE ADMINISTRATION

For sale by the Clearinghouse for Federal Scientific and Technical Information
Springfield, Virginia 22151 – CFSTI price $3.00

EXPERIMENTAL INVESTIGATION OF REACTOR-LOOP TRANSIENTS DURING STARTUP OF A SIMULATED SNAP-8 SYSTEM

by Pierre A. Thollot, Henry B. Block, and Kent S. Jefferies

Lewis Research Center

SUMMARY

Experimental investigations of primary-loop transients during the startup of a Rankine-cycle space-power system were conducted in the SNAP-8 Simulator Facility at Lewis. Of particular significance to these studies was the fact that both a realistic reactor simulator and a flight-weight mercury boiler were used in the primary loop. Furthermore, the system tested used the same liquid metals and operated at similar temperatures, pressures, and flow rates as those of the SNAP-8 system. During startup, the electric heater power input was automatically controlled so that the transient behavior of a real reactor could be duplicated. With the exception of this automic power control, all other variables were manually controlled to predefined values.

In order to evaluate the relative merits of the wide variety of startup modes studied, a method of judging the results of each run was derived based on the reactor simulator exit temperature excursion. A comparison of this criterion with individual nuclear-system constraints showed excellent agreement. Examination of the effects of a variety of primary- and power-loop flow schedules on transients in the primary loop revealed a strong interdependence on their relative shapes. When, for example, the power-loop flow schedule is fixed, it was observed that a limited range of primary-loop flow transitions existed, beyond which the results of a mismatch adversely affected the startup transient. Furthermore, it was seen that each of the temperature coefficients of reactivity associated with reactor control logic influenced key parameters during the startup transient. Specifically, (1) as the value of upper-grid-plate coefficient approached zero, the maximum reactor simulator exit temperature attained increased markedly, (2) as the absolute value of core coefficient increased, the magnitude of the first power peak decreased, and (3) as the absolute value of lower-grid-plate coefficient increased, startups with a more rapid initial rate of change of power resulted.

It was concluded that primary-loop heat capacity and how it is distributed also plays an important role during startup. In order for a simulating system to provide useful startup data, its primary-loop thermodynamic characteristics should match as closely as possible those of the nuclear-power system.

INTRODUCTION

Among the wide variety of space-power systems, those which utilize nuclear reactors cooled by liquid metals have unique problems associated with their startup. As a rule, such startups are initiated by a remote command signal and are required to be entirely automatic. Therefore, startup transients must be thoroughly studied during system development.

SNAP-8 (System for Nuclear Auxiliary Power) (ref. 1) is a Rankine-cycle space-power system consisting of three liquid-metal loops designed to generate 35 kilowatts of net electrical power. The primary-loop liquid metal, which is NaK (the eutectic mixture of sodium and potassium), transfers heat energy from a nuclear reactor to a two-phase mercury power loop through a heat exchanger, or boiler, common to the primary and power loops. After passing through a turbine, the mercury vapor is condensed, and the heat energy so released is transferred to a space radiator by means of a NaK heat-rejection loop. Startup of this type of system has two phases: (1) reactor startup during which the nuclear reactor is brought to operating temperature, and (2) power-conversion-system startup during which the power conversion system is started and the complete system is brought to full-power operation. At the beginning of this second phase, mercury is injected into the evacuated power loop for a fixed length of time and in a programmed manner. This injection process brings the turbine alternator to rated speed. When injection is completed, the alternator-powered mercury pump begins the recirculation of liquid mercury accumulating in the condenser. The mercury flow rate is then increased to the full-power value in a gradual manner. In this transition phase, there are potential operating problems in each of the three loops. Among these are the problems associated with the temperature and power transients of the nuclear reactor loop. It is during this second phase of startup that the major power transient is imposed on the nuclear reactor. In order to assure a safe transition, constraints associated with reactor operation must be met.

Although some experimental steady-state SNAP-8 nuclear-reactor data are available (ref. 2), reactor-loop transients have been studied heretofore solely by theoretical analysis and computer simulation (refs. 3 and 4). Therefore, an experimental investigation of the reactor-loop transients during startup of a three-loop liquid-metal power system simulating the SNAP-8 system was conducted at the Lewis Research Center. Of particular significance to these studies was the fact that the primary loop of the experimental power system utilized a reactor simulator (ref. 5) and a flight-weight mercury boiler. No attempt was made to duplicate the pipe dimensions of the SNAP-8 system.

Several startup modes were investigated; in each, the input power was automatically controlled by the reactor simulator over an approximate range of 35 to 415 kilowatts. The manner in which each of the following independent variables affected startup dynam-

ics was studied: the time history of both the mercury- and the primary-loop flow rates, the temperature coefficients of reactivity used in the reactor simulator, and the initial primary-loop power level. The scope of the work included four distinct mercury injection schedules, four separate groups of reactivity coefficients, four types of primary-loop flow ramps, and two values of initial reactor simulator power. Each startup began with zero mercury flow (pump power off), and was considered to end either when stable steady-state operation was achieved or when one of the several safety limits had been exceeded. A method by which the merit of each run could be evaluated, based on the reactor exit temperature excursion, was derived. Sixteen startup runs are evaluated herein.

SYMBOLS

C_p	specific heat, Btu/(lb)(^oF); J/(kg)(^oK)
F_1	primary-loop NaK flow rate, lb/hr; kg/sec
F_2	power-loop mercury flow rate, lb/hr; kg/sec
IPD	initial power deficit (integral of PWR_D-PWR_E from zero to first crossover point), kW-sec
m	weight, lb; kg
PWR_C	computed power signal of the reactor simulator, kW
PWR_D	thermal power demand including primary-loop losses, kW
PWR_E	electrical power supplied to NaK heater, kW
P_{1-8}	primary-loop electromagnetic pump inlet pressure, psia; N/m^2 abs
P_{1-9}	primary-loop electromagnetic pump outlet pressure, psia; N/m^2 abs
P_{2-1}	boiler exit mercury vapor pressure, psia; N/m^2 abs
P_{2-20}	boiler inlet mercury pressure, psia; N/m^2 abs
T_c	reactor simulator NaK heater core temperature, ^oF
TEP	reactor simulator temperature excursion parameter, (^oF)(sec); (^oK)(sec)
T_{lg}	reactor simulator NaK heater lower grid temperature, ^oF; ^oK
T_{out}	reactor simulator NaK heater outlet temperature, ^oF; ^oK
T_{1-1}	NaK heater outlet temperature, ^oF; ^oK
T_{1-3}	boiler inlet NaK temperature, ^oF; ^oK
T_{1-7}	boiler outlet NaK temperature, ^oF; ^oK

T_{1-10}	NaK heater inlet temperature, ^{o}F; ^{o}K
T_{2-1a}	boiler exit mercury vapor superheat temperature, ^{o}F; ^{o}K
T_{2-1b}	boiler exit mercury vapor saturation temperature, ^{o}F; ^{o}K
T_{2-20}	boiler inlet liquid mercury temperature, ^{o}F; ^{o}K
t	time, sec
t_1	time at which first drum step-in occurred, sec
t_2	time at which first drum step-out occurred, sec
α_c	core temperature coefficient of reactivity, ¢/^{o}F; ¢/^{o}K
α_{lg}	lower grid temperature coefficient of reactivity, ¢/^{o}F; ¢/^{o}K
α_{ug}	upper grid temperature coefficient of reactivity, ¢/^{o}F; ¢/^{o}K
δ_k	reactivity computed by simulator, ¢

APPARATUS

General Description

The SNAP-8 simulator facility (S8SF) consisted of three major loops as shown in figure 1. The primary NaK loop (equivalent to the reactor loop) transferred heat energy from the 550-kilowatt electric heater to the tube-in-shell mercury boiler. The primary loop NaK was circulated by an electromagnetic (EM) pump, and the mass flow rate was measured by an EM flowmeter. In the two-phase mercury loop (equivalent to the power loop), liquid mercury was circulated by a centrifugal pump and vaporized in the boiler. The vapor was directed through a turbine simulator and liquefied in the condenser. Mass flow rate of mercury was regulated by a pneumatically operated valve and was measured using a venturi. The NaK heat-rejection loop transferred waste heat from the condenser to two parallel air-cooled heat exchangers. Two EM flowmeters were used to measure total and condenser flow rates, and an EM pump was used to circulate the fluid. The primary-loop area including the electric heater and mercury boiler is shown in figure 2. Figure 3 is a photograph of the S8SF control panel, in which the analog computer (used in the reactor simulator) can be seen. Further details of the test equipment are given in reference 6.

Primary NaK Loop

A schematic diagram of the primary NaK loop is shown in figure 4. A closed-loop

control system consisting of the electric heater, the ignitron power controller, and the analog computer circuit logic composed the reactor simulator. As illustrated in figure 5, thermocouples physically located within the electric heater, supplied the analog computer with measurements from which a command power signal could be computed on-line and in real time. Multiplying the various internal temperatures by appropriate coefficients provided a value of reactivity due to temperature distribution. In addition, the effect of outlet temperature dead-band control on reactivity through the stepwise positioning of neutron reflectors was included. The nucleonic simulation used the total calculated reactivity to compute equivalent reactor power. By means of the power controller, heater input power was controlled to match this equivalent reactor power. The design details and the performance of the reactor simulator are discussed in reference 5. The electric heater is shown in figure 6. NaK entered the lower plenum, was distributed to channels paralleling the heating-element wells by holes in the lower grid plate, and passed out of the heater by flowing laterally through the upper-manifold region.

The tube-in-shell mercury boiler is shown in figure 7. Liquid mercury entered the header, was distributed to four tubes, and was vaporized. Each tube contained two turbulating devices: one in the liquid region and the other in the vapor region. Hot primary-loop NaK was directed in a cross counterflow manner over the outside areas of the mercury containment tubes.

Listed in table I are physical properties and changes in heat content associated with the primary loop. The last column lists typical values representative of the change in stored energy in the primary loop from prestart to full power operation.

Instrumentation and Data Recording

Instrumentation used in documenting system performance during the startup transient consisted of thermocouples, pressure transducers, flowmeters, and a power measuring circuit. The location of this instrumentation is indicated in figure 4. Chromel-Alumel thermocouples, referenced to 150° F (338.7° K), were used to measure internal NaK heater temperatures, heater inlet and outlet temperatures, and all boiler temperatures. Pressure measurements were made using commercial instruments where the high-temperature sensing diaphragm was separated from the bourdon-tube - electronic transducer by a slender NaK filled tube. Primary- and heat-rejection loop flows were measured using EM flowmeters. The mercury flow rate was measured using a calibrated venturi in the liquid line at the boiler inlet. Electrical power supplied to the heater was continuously calculated by electronic multipliers and used in the feedback circuit of the ignitron controller (see fig. 5). A more detailed description of the instrumentation is given in reference 7.

Data from these instruments were converted to digital form and stored on magnetic tape using CADDE (Central Automatic Digital Data Encorder, ref. 8). The coded data from CADDE was fed to a digital computer, which was programmed to produce time-history plots and a tabulation of computed results.

For continuous monitoring of key parameters, a six-channel pen recorder was used. Recorded in this manner were the analog computer calculation of excess reactivity, reactor simulator command power, the mercury flow venturi ΔP, and three of the NaK heater temperatures that were used to compute equivalent reactor power.

TEST PROCEDURE

A brief description of the mechanics of a physical startup, system limitations, and a summary of the test program is presented in the following sections.

Typical Startup Procedure

Each run began with the primary-loop NaK flow at approximately 16 000 pounds per hour (7260 kg/hr) (50 percent of S8SF rated value), a heater outlet temperature of 1300° F (977.6° K) (nominal S8SF rated value), the heater power in manual control and at a value sufficient to maintain the required 1300° F (977.6° K) outlet temperature. In the mercury power loop, all liquid lines between the condenser outlet and the boiler inlet were prefilled, the condenser was partially filled, the flow-control valve was closed, and the mercury pump power was off. When the prestart checkout was completed, the mercury pump power was turned on and the flow-control valve was slowly opened. Time zero was defined as the time at which the first indication of mercury flow was obtained. Shortly after time zero, control of the electric heater input power was switched to the reactor simulator and remained there until the run ended. Manual control of the NaK and mercury flow rates was achieved by comparison of control meter read-outs with predefined requirements as a function of running time. Conditions in the heat-rejection loop were manually controlled such that the condenser NaK inlet temperature remained around 500° F (533° K) and the condenser mercury inlet pressure was between 12 and 14 psia (8.27 and 9.65 N/cm^2). Critical primary-loop parameters were monitored throughout the startup on a six-channel pen recorder.

Each run ended either in successful steady-state operation or as a result of having exceeded one of the S8SF safety limits. Typical steady-state values attained were electric heater input power, 420 kilowatts; primary-loop NaK flow rate, 32 500 pounds per hour (14 740 kg/hr); and power-loop mercury flow rate, 9300 pounds per hour (4220 kg/hr).

Several continuously monitored parameters were provided with safety limits which were interlocked in such a way as to terminate system operation when tripped. Those in the primary loop included heater outlet temperature (1375° F or 1019° K) and electric heater power (475 kW).

System Limitations

Startup studies were scheduled as the last phase of the S8SF test program. Because of problems with test support equipment, limitations were encountered which affected testing. Primary-loop NaK flow, for example, was limited to 32 500 pounds per hour (14 740 kg/hr) as a result of EM pump degradation; breakdown of winding insulation was later found to be the principal problem. Mercury flow control was difficult especially at low flow rates because the pneumatically operated control valve had to be manually positioned. An electrohydraulic controller had been installed on this valve; however, during previous tests, it had failed and was replaced. These and other system problems are discussed in more detail in reference 6.

Summary of the Test Program

Considerable flexibility existed in the type and range of independent variables tested. As a result, a variety of startup modes was investigated. The prime independent variable was mercury flow schedule. Because of the method of flow control, it was not always possible to obtain exactly the desired flow schedule. In the SNAP-8 system the mercury flow schedule defines the NaK flow schedule because of the interrelation of the initial mercury flow rate, turbine acceleration, alternator frequency, and primary NaK pump speed. In general, for the tests performed, the primary-loop NaK flow schedule called for was the anticipated flow transition of a SNAP-8 system having the particular mercury flow prescribed for each test. With the SNAP-8 reactor nucleonics and control logic simulated on an analog computer, the test program was able to include as independent variables (1) temperature coefficients for lower grid plate, core, and upper grid plate, (2) control-drum-step worth, and (3) initial reactor power level. The value of reactor outlet temperature control dead-band limits (high, 1320° F (988° K); low, 1280° F (966° K)) and the time interval between successive drum steps (220 sec) remained unchanged for all runs.

To simplify the presentation of the combination of variables that constituted each test run, figure 8 and tables II and III are presented. The prescribed mercury-loop and primary-loop NaK flow schedules used are illustrated in figure 8. The values used for each of the temperature coefficients in the reactor simulator model are listed in table II.

The choice of temperature coefficients was arbitrary with the exception of group D which was experimentally selected based on the smoothest temperature and power transients resulting from a 25-percent step change in either mercury or NaK flow while at 375-kilowatt operation. Table III lists the combination of variables used in each test.

METHOD OF DATA EVALUATION

Examination and evaluation of experimental data of this type present a problem, in that there exists no absolute criteria for judging the merit of individual startups. In reality, only the boundaries are well defined, namely, achievement of steady-state operation at one extreme, and at the other, premature termination either because of a failure or because one of the S8SF safety limits was exceeded. In this section, basic nuclear-system constraints are examined, and a method for judging the relative merit of individual startups is presented.

Reactor Constraints

Starting the power (mercury) loop of a Rankine cycle space-power system imposes a severe transient on the reactor. Specifically, the manner in which mercury is introduced to the boiler determines the rate at which power is removed from the primary NaK loop. To satisfy this power demand, the reactor responds to a drop in coolant temperature in two ways, each of which increases reactivity. Besides the dead-band control discussed earlier, the reactor is constructed such that, as the coolant temperature decreases, small variations in physical configuration occur which contribute to the change in reactivity which, in turn, causes an increase in reactor power. To keep the startup transient within limits that assure safe nuclear reactor operation, constraints have been defined. Those constraints which apply directly to startup are

(1) Maximum thermal power

(2) Maximum reactor outlet temperature

(3) Minimum reactor inlet temperature

(4) Maximum time rate of change of reactor coolant temperature

These limitations reflect reactor-scram conditions and thermal stress considerations. Therefore, in evaluating the performance of different startup modes, it would first be necessary that none of the constraints be exceeded. Following this determination, it would be necessary to compare the severity of individual startup transients. Prior to evaluating the results of the startups reported herein, a method by which the startup severity could be gaged had to be derived.

Scale of Merit

In considering what parameter or combination of variables to use for evaluation of individual startups, it became evident that guidelines were required. The guidelines chosen were that

(1) the parameter should be directly related to the basic primary-loop constraints mentioned earlier

(2) the effects related to each of the independent variables studied should be reflected in the parameter chosen

(3) the parameter should be indicative of system transient behavior

The variable chosen on which to judge individual startups was the time integral of the reactor coolant-exit temperature during its first excursion above the upper dead-band limit of 1320° F. Hereinafter this variable will be referred to as the temperature excursion parameter (TEP), which is measured in $^{\circ}$F-sec ($^{\circ}$K-sec). Sketch (a) illustrates the TEP variable.

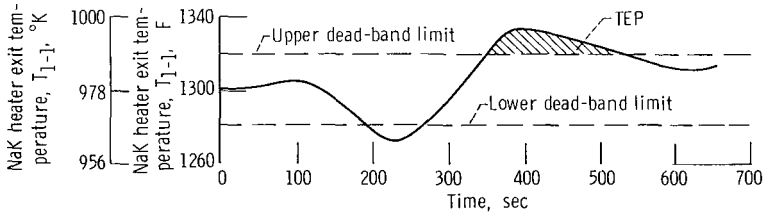

(a)

Based on the value of TEP for each of the runs that achieved steady state, an arbitrary scale of merit was defined so that all such runs fell in the range from 5 to 10, with 10 being the best. Run 1, which had the largest TEP value, was assigned a merit value of 5, and run 8, which had the smallest value of TEP, was assigned a merit value of 10. A straight line was drawn between these two points and the remainder of the runs were assigned values of merit based on their value of TEP and this line. Because of the arbitrary nature of this assignment, only whole numbers were used for values of run merit. Figure 9 is the graphical result. By definition then, test run 1 (see fig. 9) was the poorest of those which achieved steady state, and run 8 was the best. For those runs which did not reach steady state (i.e., exceeded one of the safety limits), the startup terminated before a value for TEP was defined. Because it was desirable to evaluate data from all runs made, a compromise was necessary in order to extend the scale of merit from 5 down to 1. As before, the smaller the value of merit, the poorer the run.

In order to accomplish this extrapolation, a variable was needed that correlated well with TEP for all runs successfully achieving steady state and that could be evaluated for those runs which terminated early. After examination of all the available data the initial power deficit (IPD) was found to exhibit characteristics similar to those of TEP. The IPD is defined as the time-integral of the difference between the power demanded and the thermal power supplied up to the first crossover point. Power demand is defined as that power required to vaporize all the mercury entering the boiler and raise it to the temperature attained at steady state, plus the heat loss associated with the primary loop. Sketch (b) illustrates the area which constitutes the IPD.

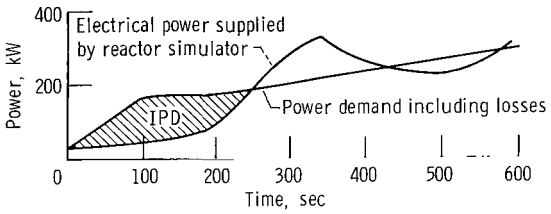

(b)

Plotting IPD as a function of the scale of merit (as previously defined by TEP) for those runs which achieved steady state showed good correlation (see fig. 10). This result was used to extend the scale of merit down to a value of one for those runs which terminated early. In effect, assuming the relation between TEP and IPD can be extrapolated, a scale of merit based on the reactor simulator exit temperature excursion parameter was assigned to all runs. Two exceptions to the general rule were required and are not shown in figure 10. Run 11 was by far the poorest run made because the combination of mercury flow schedule, reactor coefficients, and primary-loop configuration represented an unrealistic system (i. e., the power demand increased to a maximum before the power supplied had a chance to catch up). For this reason run 11 was assigned a merit value of 1. Run 16 was also an exception, in that the reactor temperature coefficient for the upper grid plate was set to zero (i.e., no contribution to the power command signal was introduced by coolant temperature changes in the upper grid plate region). This together with the mercury flow schedule used resulted in a run which had to be manually terminated before the NaK heater outlet temperature recrossed the upper dead-band limit. Having effectively no feedback on outlet temperature resulted in this temperature remaining well above the upper dead band for too long a period of time (maximum value 1370° F (1016° K)). As a result. the run was intentionally halted. The effect of successive drum steps during this time interval would eventually have brought the

temperature down, but it would have taken too long and resulted in a very oscillatory startup. The method used to assign a value of merit to run 16 will be discussed later.

The effectiveness of the temperature excursion parameter was evaluated by plotting the scale of merit (as determined by TEP) as a function of each of the reactor constraints mentioned earlier. In order to make a meaningful comparison, runs 1 to 8, which all had the same temperature coefficients of reactivity and therefore represented the same reactor model, were selected. From the comparisons shown in figure 11, it can be seen that higher figures of merit coincide with improved system performance based on individual reactor-loop constraints. (Note that data plotted represent runs made with various NaK flow schedules, initial powers, and mercury flow schedules, see table III.) The second plot in figure 11 was used to assign a figure of merit to test run number 16 and represents an exception to the general rule.

RESULTS AND DISCUSSION

Included in this section is a description of typical data, a discussion of the effects of each of the variables studied, and an examination of the power transient.

Typical Data

Data from two sources were used in this analysis. The previously described central digital system, which recorded each data channel every 18.6 seconds, produced machine plots of selected variables. A control room pen recorder was used to record six variables that allowed on-the-spot monitoring of the startup transient. Examples of digital data and pen recorded data for run 8 are shown in figure 12. The same variables for run 11, considered to be the poorest of the runs made, are shown in figure 13. It was from plots of this type that all results were obtained. In order to simplify the presentation of data for all runs made, 25 key parameters were selected for tabulation. In figure 14, each of the 25 parameters is defined and illustrated for data results of run 5. The tabulation of these data along with the figure of merit, reactor simulator temperature coefficients, and flow rate schedules used for each of the runs reported appear in table IV.

In experimentation of this kind, one measure of the validity of the data is how well it can be repeated. In figure 15, data from two runs, run 9 and a repeat test (run 10), illustrate the excellent repeatability.

Effect of Initial Reactor Simulator Power

A principal dynamic characteristic of the SNAP-8 nuclear reactor, also present in the simulator, is that the time constant associated with power changes is inversely proportional to the absolute value of neutron flux (power level). It follows that the higher the initial value of power, the easier it will be for the reactor to respond to startup transients. In effect, the control sensitivity increases as the operating power level rises. In the SNAP-8 system, an auxiliary start loop allows some primary-loop power to be transferred to the heat-rejection loop directly, prior to power-loop startup. This feature was not available in the S8SF test loop. As a result, only slightly higher initial power levels than were necessary to supply primary-loop losses could be tested. Two test runs (runs 5 and 6) identical in all respects except initial power may be compared. Examination of individual TEP values reveals that the run with the higher initial power had a smaller value of TEP, indicating an improved startup. However, because only whole numbers were used for the scale of merit, the two runs in question received the same figure of merit.

Effect of Temperature Coefficients of Reactivity

Using a reactor simulator allowed the test program to include as independent variables the values of temperature coefficients of reactivity. A brief discussion of these coefficients and their significance is in order. As mentioned previously, the nuclear reactor used in the SNAP-8 system is constructed such that the configuration (and, hence, the reactivity) changes with temperature to produce a negative feedback. As an example, the upper and lower grid plates, which support the fuel element bundle, contract as temperature decreases. This contraction results in higher reactivity within the reactor. A simple representation of the primary-loop logic, including control characteristics applicable to both the reactor simulator tested and a reactor-powered system, is presented in block form in figure 16. The thermodynamic logic shown by the solid line in the figure, represents the heat-transfer loop including the NaK heater (reactor), the boiler, the piping between them and the NaK flowing through the loop. The NaK heater was broken into four blocks to show the relations of the various temperatures that have feedback effects. The inherent reactor control is represented by the three loops containing the temperature coefficients of reactivity α_{lg}, α_{c}, and α_{ug}. The dead-band control of outlet temperature mentioned earlier introduces step changes of reactivity as the outlet temperature crosses either of the dead-band limits.

From the data recorded during the startup studies, it was possible to isolate the principal effects of each of the temperature coefficients of reactivity. It should be noted that,

in all runs used for this comparison, all other independent variables remained essentially unchanged. The upper-grid-plate coefficient α_{ug} has its greatest effect on NaK exit temperature. As the coefficient (i. e., gain) associated with changes in reactivity due to changes in exiting NaK temperature varies, so, too, does the maximum value attained by the exit temperature. Data from runs 5, 10, and 16 presented in figure 17(a) illustrate this result. As the value of upper-grid-plate coefficient approaches zero, startups with higher values of outlet temperature result. The core temperature coefficient α_c has a noticeable effect on the first peak in power. Figure 17(b) illustrates that more severe power overshoots occur as the value of core temperature coefficient approaches zero. In both cases (fig. 17(a) and (b)), increasing the absolute value of the coefficient causes a decrease in the dependent variable which, in turn, reduces the overall system transient. The lower-grid-plate coefficient α_{lg} strongly influences the initial rate of change of power as shown for two sets of data in figure 17(c). Increasing the absolute value of α_{lg} results in a higher power level at the time of the first drun step-in. This is beneficial in that it makes the power more responsive to changes in reactivity during the early phases of the startup transient.

Interpreting the results of figure 17 in terms of the block diagram in figure 16 shows that (1) initial inherent control action results from a change in inlet temperature and is related to α_{lg}, (2) the first power peak is affected by the inner-feedback loop and is related to α_c, and (3) outlet temperature stabilization is introduced by the outer-feedback loop and is related to α_{ug}. Furthermore, increasing the sum of the absolute values of the three temperature coefficients tends to improve the dynamic behavior of runs similar in all other respects (fig. 18).

Effect of Primary-Loop Flow Schedule

Before discussing the results of various primary-loop flow transitions, a brief examination of predicted effects for extreme cases is presented. For a given system with a fixed mercury flow schedule and a defined primary flow ramp rate, the extremes are as follows:

(1) If the transition from 50 to 100 percent of rated flow occurs very late in the start cycle, the result would be an early and rapid decrease in reactor coolant inlet temperature. This, in turn, would lead to an excessive rate of change of power and conceivably a dangerously high power overshoot.

(2) If the primary loop were ramped from 50- to 100-percent flow very early in the start cycle, the reactor coolant inlet temperature would decrease little, if at all, during the first part of the start cycle. This would result in little, if any, primary-loop power increase, while the mercury loop would continue to increase its power level. This mismatch in powers would unquestionably result in severe transients.

Examination of the startup data recorded provided examples approaching each of these cases. Run 2 is an example of late primary-loop transition, and run 3 is an example of early transition (see table III and fig. 8). These runs, as well as run 4, are similar in all respects except primary-loop flow schedule and are compared in figure 19. In drawing the curve through these data (fig. 19), the predicted extremes were assumed to exist. Examination of the figure suggests that an optimum time exists at which the primary flow ramp should begin (based on increasing scale of merit).

In one of the possible SNAP-8 system startup modes, the primary-loop pump motor is accelerated from 50- to 100-percent speed by virtue of being powered by the turbine alternator as it accelerates from 50 to 100 percent of rated speed (see Summary of Test Program section). This procedure, of course, would not necessarily result in the optimum discussed previously. However, in the majority of tests performed, a primary-loop flow schedule similar to that anticipated by a turbine alternator powered pump was used, with no apparent problem.

Effect of Mercury Flow Schedule

Because of the way in which mercury flow was controlled, the shape of the F_2 curve at low flow rates did not always conform to the desired schedule. To account for this fact in evaluating the results, a fixed injected inventory (i. e., area under the flow rate against time curve) was selected as the independent variable to be studied. Hence, the time required to inject 92 pounds (an arbitrary choice) of mercury was determined for each run (see table IV) and used as an indication of initial mercury flow schedule. In a previous work (ref. 3), it was concluded that the rate of change of mercury flow during the first 100 to 200 seconds is most critical. The effects related to the remaining portion of the mercury flow schedule are not considered.

In reference 3, it was concluded that, if the initial mercury ramp rate was extremely steep, the resulting primary-loop transients would be excessively severe. On the other hand, if the mercury injection schedule and corresponding primary-loop flow transition was very flat and extended for a long period of time, the resultant startup would be slow and well behaved. It would be expected, therefore, that a plot of the time required to inject 92 pounds (42 kg) of mercury as a function of the scale of merit would show that, as this time increased, improved startups result.

Such a plot (fig. 20) was made for the normal runs which utilized group D coefficients (runs 1 and 2 were not included because of the atypical nature of the primary NaK flow schedule, see fig. 8). Examination of figure 20 indicates the expected result (solid line) in all cases but one. A careful examination of runs 7 and 8 reveals that all independent variables were alike except the mercury flow rate. The reason that run 7, with a more

gradual initial mercury flow ramp than run 8, does not have a higher figure of merit is evident when the discussion associated with primary-loop flow schedule is recalled. This discussion brought out that proper matching of primary and mercury flows must exist. In run 7, however, a gradual mercury ramp rate was matched to the same primary flow schedule used for the more rapid mercury ramp rate of run 8. It is concluded that the results of a series of runs in which all independent variables except mercury flow schedule were held constant would resemble the dashed line extrapolation of figure 20. These data again point out the strong interdependency that exists between primary- and power-loop flow schedules during the startup transient.

Power Transients

Two parameters of interest during startup are power demand (directly related to mercury flow schedule) and power supplied by the reactor (indirectly related to primary-loop NaK temperatures). In an earlier section (Effects of Temperature Coefficients of Reactivity), some of the control logic associated with primary-loop temperature effects on power were discussed (see fig. 16). A system parameter which affects the dynamic behavior of these temperatures is the magnitude and distribution of primary-loop heat capacity. A graphic picture of startup dynamics is afforted when both power parameters are plotted on the same graph. Figure 21 is typical of the results obtained and illustrates the dynamic power imbalance which the system undergoes. The results of run 8 (fig. 21(a)) and run 4 (fig. 21(b)) illustrate two cases: one in which a small power overshoot occurred and one in which a larger overshoot occurred. The large power mismatch evident in run 4 is characteristic of the poorer runs. In fact, the relative merit of each startup could be approximately predicted from an examination of the power transient. Furthermore, the difference between the total area under the power-demand curve and that under the power-supplied curve represents the heat energy absorbed due to the change in temperature of various portions of the primary loop. A comparison was made between typical values obtained graphically from plots like those in figure 21 and the calculated results of the change in primary-loop stored energy as illustrated in table I. In the graphical analysis, it was assumed that 100-percent mercury quality existed at the boiler exit throughout the startup and that an inventory of 100 pounds (45.36 kg) of liquid mercury remained in the boiler at the end of the startup. Typical graphical results indicated approximately 18 500 Btu (19.5×10^6 J) as compared with 21 300 Btu (22.45×10^6 J) from table I.

If it is assumed that the most important period in startup occurs during the first several hundred seconds, the initial power deficit (IPD) and the secondary power excess (SPE) illustrated in figure 21(b) become important parameters. The first area, IPD,

aside from being directly affected by each of the independent variables studied, also reflects the delaying action introduced by the primary-loop heat capacity. For this reason, the IPD can never have a value of zero. The difference between IPD and SPE represents the portion of the primary-loop stored energy absorbed by the system during the early stages of startup. The ratio of SPE to IPD is indicative of the oscillatory nature of the power transient. By induction (ref. 8), it was reasoned that the absorbed energy, weighted by the ratio of SPE to IPD, should be related to startup merit.

In order to check this hypothesis, calculated results of this relation were plotted as a function of the average value of the temperature excursion parameter (TEP divided by the time period associated with TEP). The plot is shown in figure 22; all runs which achieved steady state are included. From this figure it appears that a correlation exists between the power parameter $\left|(\text{IPD} - \text{SPE})(\text{SPE}/\text{IPD})\right|$ and the average value of the temperature excursion. Furthermore, the sensitivity (slope), which relates these two parameters, has the units of Btu/^{o}F (J/^{o}K). This result tends to indicate that the sensitivity of reactor exit temperature excursions to power excursions is related to heat capacity. Further studies are needed to define this relation for systems with different heat capacities. It can be concluded, however, that, in order to perform realistic startup studies, differences between test and reference-system primary-loop configurations must be kept to a minimum.

CONCLUSIONS

Startup studies of a SNAP-8-type system were performed to define the principal effects of key independent variables on the thermal transients of the primary (nuclear) loop. The primary loop contained a reactor simulator and a flight-weight mercury boiler. Independent variables which were studied include initial reactor power, both primary NaK and mercury flow-rate schedules, and the temperature coefficients of reactivity of the reactor model. In evaluating the results of each startup transient, it was necessary to derive a scale of merit. The variable chosen on which to base the relative merit of each run was the area enclosed by the reactor simulator coolant exit temperature during its first excursion above the upper dead-band limit. This variable, defined as the temperature excursion parameter proved to be a good indication of overall system behavior during the startup transient, based on existing reactor-loop constraints. The conclusions drawn from the test were as follows:

1. For a fixed mercury flow schedule there exists a range of times for primary-loop flow transition from 50 to 100 percent of rated flow that most effectively matches the given mercury schedule. The matching afforded by driving the primary loop pump with the turbine-alternator was simulated and revealed no apparent problems.

2. For tests in which the primary-loop flow transition used simulated coupling of the primary-loop pump with the turbine alternator, it was found that, as the time required to inject a fixed amount of mercury increased, the resulting startup transients were less severe based on the temperature excursion parameter.

3. The following conclusions were drawn concerning the temperature coefficients:

a. The upper-grid-plate temperature coefficient of reactivity had its greatest effect on reactor outlet temperature excursions. As it approached a value of zero, dangerously high values of outlet temperature were encountered.

b. The core temperature coefficient of reactivity noticeably effected the first peak in reactor power. Increasing the magnitude of this coefficient resulted in less severe power overshoots.

c. The lower-grid-plate temperature coefficient of reactivity strongly influenced the initial rate of change of reactor power. Increasing the magnitude of the coefficient increased the initial rate of change of power and, therefore, resulted in a higher power level at the time of the first action of the dead-band control. This, in turn, increased the effectiveness of the control action.

d. Increasing the magnitude of the sum of temperature coefficients of reactivity improved the startup transient based on the temperature excursion parameter.

4. Primary-loop transients were somewhat less severe for startups with higher values of initial reactor power.

The effect of primary-loop heat capacity and how it is distributed, although not treated as an independent variable, is considered to strongly influence the overall system behavior during startup. For meaningful startup studies, primary-loop thermodynamic characteristics should match as closely as possible those of the reactor-powered system.

Lewis Research Center,
National Aeronautics and Space Administration,
Cleveland, Ohio, December 1, 1967,
701-04-00-02-22.

REFERENCES

1. Anon.: AIAA Specialists Conference on Rankine Space Power Systems. Vol. 1. AEC Rep. No. CONF-651026, Vol. 1, 1965.

2. Fead, L. M.; Felten, L. D.; and Rooney, V. L.: SNAP 8 Experimental Reactor Operations and Test Results. Rep. No. NAA-SR-10903, Atomics International Div., North American Aviation, June 28, 1965.

3. Birken, S.: Response of the SNAP 8 Reactor During Automatic Startup. Rep. No. NAA-SR-9646, Atomics International Div., North American Aviation, Sept. 24, 1964.

4. Code, C. J., Jr.: Analysis of the Response of the SNAP 8 Nuclear System During Startup of the Power Conversion System. Rep. No. NAA-SR-9626, Atomics International Div., North American Aviation, June 8, 1964.

5. Jefferies, Kent S.; Packe, Donald R.; and Dittrich, Ralph T.: Design and Performance of a Nuclear Reactor Simulator for Nonnuclear Testing of Space Power Systems. NASA TN D-4095, 1967.

6. Valerino, Alfred S.; Wood, James C.; and Reznik, Joseph F.: SNAP-8 Simulator Loop Mechanical Design. NASA TM X-1515, 1968.

7. Deyo, James N.; and Wintucky, William T.: Instrumentation of a SNAP-8 Simulator Facility. NASA TM X-1525, 1968.

8. Staff of Lewis Research Center: A Central Facility for Recording and Processing Transient-Type Data. NASA TN D-1320, 1963.

9. Mill, John Stuart: System of Logic. Longmans, Green and Co., 1930, pp. 222-237.

TABLE I. - PRIMARY-LOOP THERMODYNAMIC PROPERTIES WHICH AFFECTED STARTUP

[Electromagnetic pump heat input was considered equal to system heat loss. Heat input from insulation was considered negligible.]

Location	Weight, m		Specific heat, C_p		Heat capacity, mC_p		Regional average temperature change, ΔT		Change in heat storage, $mC_p \Delta T$	
	lb	kg	$\frac{Btu}{(lb)(^oF)}$	$\frac{J}{(kg)(^oK)}$	$\frac{Btu}{^oK}$	$\frac{J}{^oK}$	F^o	K^o	Btu	J
Electric heater										
Lower region										
Shell	319	145	0.120	500	38.3	72 387	133	73.9	5094	5348 $\times 10^3$
Heater rods	334	152	.157	654	52.4	99 036	77	42.8	4035	4237
NaK inventory	25	11	.211	879	5.28	9 979	121	67.2	639	671
Upper region										
Shell	319	145	.120	500	38.3	72 387	46	25.5	1762	1850
Heater rods	334	152	.157	654	52.4	99 036	-29	-16.1	-1520	-1596
NaK inventory	25	11	.211	879	5.28	9 979	51	28.3	269	282
Piping from electric heater to mercury boiler	19	8.6	.120	500	2.28	4 309	-9	-5.0	-20	-21
NaK inventory in piping from electric heater to mercury boiler	6	2.7	.211	879	1.27	2 400	-9	-5.0	-11	-11.6
Mercury boiler										
Upper region										
Shell and tubes	436	198	.120	500	52.3	98 847	34	18.9	1778	1867
NaK inventory	70	32	.211	879	14.8	27 972	34	18.9	503	528
Mercury inventory	---	-----	-----	---	-----	------	---	----	-----	----------
Lower region										
Shell and tubes	436	198	.120	500	52.3	98 847	119	66.1	6224	6535
NaK inventory	70	32	.211	879	14.8	27 972	119	66.1	1761	1849
Piping from mercury boiler to electric heater	26	12	.120	500	3.12	5 897	163	90.6	509	534
NaK inventory in piping from mercury boiler to electric heater	9	4.1	.211	879	1.90	3 591	163	90.6	310	326
Total									21 333	22.4$\times 10^6$

TABLE II. - REACTOR SIMULATOR TEMPERATURE COEFFICIENTS

Group	Temperature coefficient of reactivity						Drum step worth, ¢
	Lower grid, α_{lg}		Core, α_c		Upper grid, α_{ug}		
	¢/°F	¢/°K	¢/°F	¢/°K	¢/°F	¢/°K	
A	-0.059	-0.106	-0.048	-0.086	-0.067	-0.121	3.00
B	-.100	-.180	-.100	-.180	0	0	3.00
D	-.084	-.151	-.140	-.252	-.070	-.126	4.20
E	-.030	-.054	-.040	-.072	-.050	-.090	3.00

TABLE III. - INDEPENDENT VARIABLES FOR EACH STARTUP

Run	Power-loop mercury flow-rate schedule (see fig. 8)	Primary-loop NaK flow-rate schedule (see fig. 8)	Reactor simulator temperature coefficient (see table II)	Initial electrical power supplied to NaK heater, PWR_E, kW
1	a	e_1	D	32
2	a	e_2	D	32
3	a	a	D	35
4	a	b	D	35
5	b	b	D	53
6	b	c	D	36
7	d	d	D	50
8	c	d	D	52
9	b	b	E	50
10	b	b	E	52
11	d	c	E	50
12	c	b	E	50
13	a	a	A	36
14	a	a	A	36
15	a	a	B	35
16	b	b	B	53

TABLE IV. - SNAP-8 SIMULATOR FACILITY STARTUP STUDIES

[See fig. 14.]

Run	Scale of merit	Reactor simulator temperature coefficients	Power-loop flow-rate schedule	Primary-loop flow-rate schedule	1 Initial electrical power supplied to NaK heater, PWR_E, kW	2 Initial NaK heater outlet temperature, T_{1-1}		3 Number of drum steps	4	5 Time at which first drum step-in occurred, t_1, sec	6 Differential time, $t_2 - t_1$, sec	7 Electrical power supplied to NaK heater, PWR_E, kW, at -	8	9 Maximum rate of change of power supplied, $\Delta PWR_E/\Delta t$, kW/sec	10 Reactivity, δk, ¢, at -	11	12 NaK heater inlet temperature at t_1, T_{1-10}		13 NaK heater inlet temperature at t_2, T_{1-10}	
						°F	°K	In	Out			t_1	t_2		t_1	t_2	°F	°K	°F	°K
	(a)	(b)	(c)	(c)							(d)									
1	5	D	a	e_1	32	1307	981	1	4	226	92	110	430	5.0	14.0	6.3	1201	923	1171	906
[e]2	4			e_2	32	1301	978		--	190	---	85	---	5.7	14.0	---	1190	916	----	---
3	6			a	35	1305	980		4	180	117	96	435	4.6	13.3	3.5	1212	929	1174	908
4	7			b	35	1303	979		3	192	123	82	420	4.0	11.2	2.8	1212	929	1174	908
5	9		b	b	53	1294	974		3	192	145	100	330	2.4	8.4	2.8	1220	933	1187	915
6	9		b	c	36	1296	975		4	180	127	98	348	3.0	11.2	3.5	1212	929	1190	916
7	7		d	d	50	1297	976	None	3	NA[f]	476	NA[f]	485	3.2	NA[f]	7.0	NA[f]	---	1124	880
8	10		c	d	52	1303	979	None	3	NA[f]	416	NA[f]	360	1 75	NA[f]	4.2	NA[f]	---	1168	904
[g]9	7	E	b	b	50	1300	978	1	1	208	272	74	425	2.0	4.0	4.0	1220	933	1156	898
10	7		b	b	52	1300	978		3	200	284	72	415	1.8	4.0	3.6	1220	933	1158	899
[e]11	1		d	c	50	1303	979		--	350	---	75	---	5.0	5.8	---	1198	921	----	---
[e]12	4		c	b	50	1298	967		--	230	---	65	---	2.6	3.5	---	1220	933	----	---
[e]13	2	A	a	a	36	1296	975		--	195	---	--	---	3.1	6.0	---	1225	936	----	---
[e]14	3	A	a	a	36	1306	981		--	186	---	78	---	3.7	8.0	---	1210	928	----	---
[e]15	2	B	a	a	35	1307	981		--	204	---	100	---	4.8	10.0	---	1200	922	----	---
[h]16	2	B	b	b	53	1300	978		3+	194	137	115	380	2.3	7.0	7.2	1223	935	1188	915

Run	14		15		16		17		18		19	20	21	22	23		24	25	
	Maximum initial rate of change of heater inlet temperature, $\Delta T_{1-10}/\Delta t$		NaK heater outlet temperature, T_{1-1}				Initial rate of decrease in NaK heater outlet temperature, $\Delta T_{1-1}/\Delta t$		Maximum rate of increase in NaK heater outlet temperature, $\Delta T_{1-1}/\Delta t$		Time interval heater outlet temperature outside of --, sec		Initial power deficit, IPD, (kW)(sec)	Secondary power excess, SPE, (kW)(sec)	Temperature excursion parameter, TEP		Time required to inject 92 lb (42 kg) mercury, t, sec	Run time, sec	Startup presented in figure --
			Minimum		Maximum														
	^{o}F sec	^{o}K sec	^{o}F	^{o}K	^{o}F	^{o}K	^{o}F/sec	^{o}K/sec	^{o}F sec	^{o}K/sec	Lower dead band	Upper dead band			(^{o}F)(sec)	(^{o}K)(sec)			
1	1.0	0.556	1268	960	1354	1008	0.37	0.206	1.0	0.556	110	548	29.00×10^3	11.90×10^3	7.81×10^3	4.34×10^3	150	1280	--
[c]2	1.0	.556	1260	955	----	----	.85	.472	1.1	.613	72	---	29.00	---------	---------	---------	122	280	--
3	.85	.472	1275	964	1346	1003	.29	.161	.89	.494	62	517	24.20	12.48	6.37	3.54	116	1300	--
4	.60	.334	1273	963	1344	1002	.45	.250	.90	.500	70	300	23.00	12.00	4.51	2.51	138	920	--
5	.50	.278	1270	961	1332	995	.30	.167	.60	.334	75	200	14.05	9.49	1.72	.96	168	1045	14
6	.60	.334	1270	961	1338	999	.40	.222	.75	.416	74	230	16.50	12.80	2.36	1.31	148	1325	--
7	.80	.445	1287	970	1339	999	.25	.139	.65	.361	None	295	25.30	4.57	4.85	2.69	244	1222	--
8	.60	.334	1282	968	1330	994	.35	.194	.40	.222	None	180	16.40	2.69	.91	.51	197	1120	12
[g]9	1.0	.556	1265	958	----	---	.30	.167	.55	.306	200	---	25.10	---------	---------	---------	165	500	15
10	.85	.472	1264	958	1342	1001	.45	.250	.63	.350	215	286	24.20	13.21	5.23	2.91	180	1710	15
[e]11	.75	.416	1250	950	----	----	.35	.194	.60	.334	180	---	47.40	---------	---------	---------	268	490	13
[e]12	.65	.361	1256	953	----	----	.30	.167	.65	.361	215	---	29.50	---------	---------	---------	200	468	--
[e]13	.70	.389	1260	955	----	----	.34	.189	.62	.344	164	---	---------	---------	---------	---------	---	362	--
[e]14	.75	.416	1264	958	----	----	.30	.167	.85	.472	110	---	31.80	---------	---------	---------	128	330	--
[e]15	.95	.528	1264	958	----	----	.35	.194	.90	.500	100	---	33.50	---------	---------	---------	140	312	--
[h]16	.60	.334	1274	963	1370	1016	.40	.222	.70	.389	55	[i]718	14.70	21.56	[i]22.1	12.28	145	850[i]	--

[a] 1 worst, 10 best.
[b] See table II.
[c] See fig. 8.
[d] For runs 7 and 8 value listed is t_2.
[e] Automatically terminated prior to completion.
[f] Not applicable.
[g] T_{1-1} upper limit set too low causing accidental shutdown.
[h] T_{1-1} was running too high too long; run was intentionally halted.
[i] Estimate.

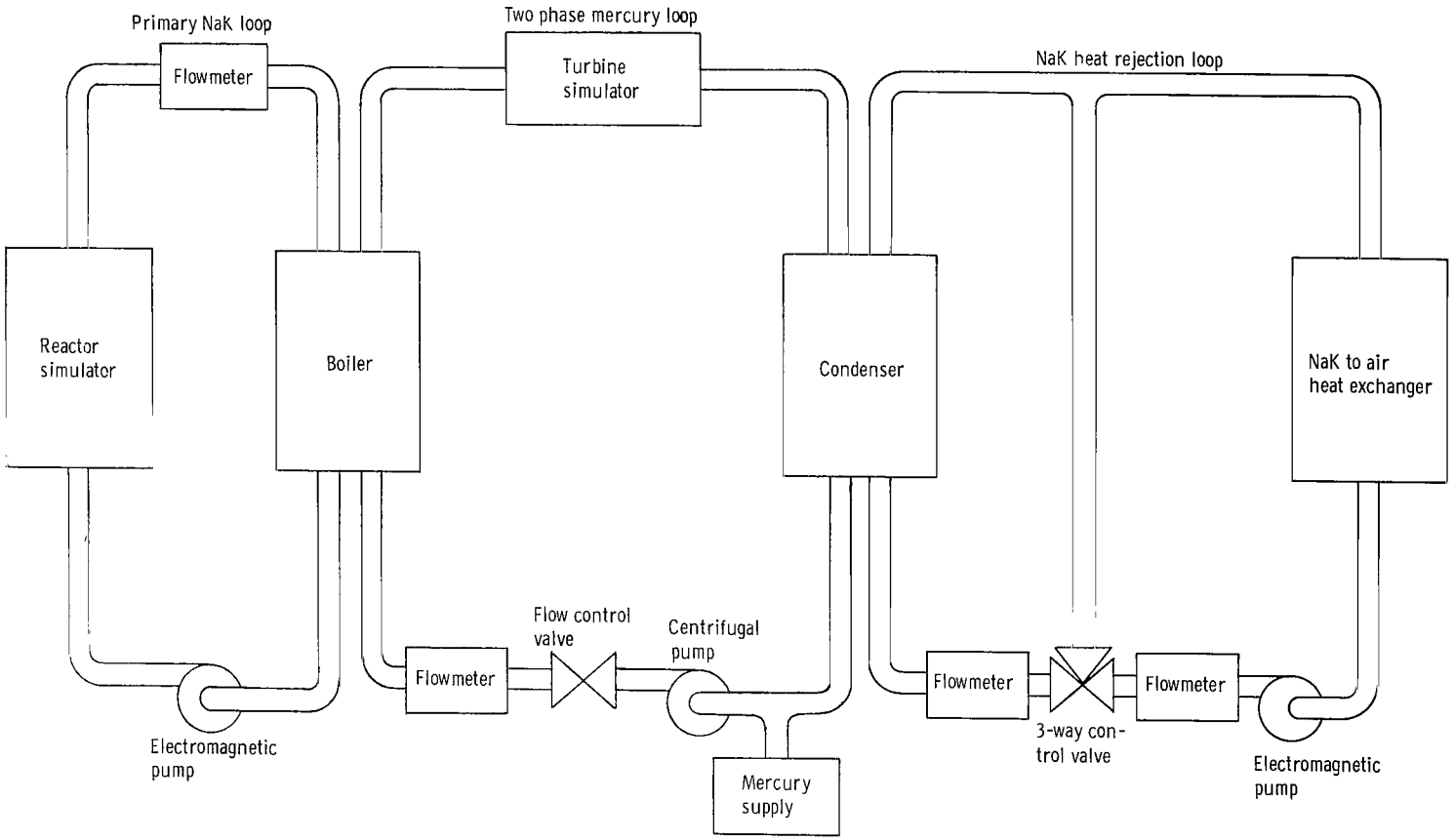

Figure 1. - Simulator loop schematic.

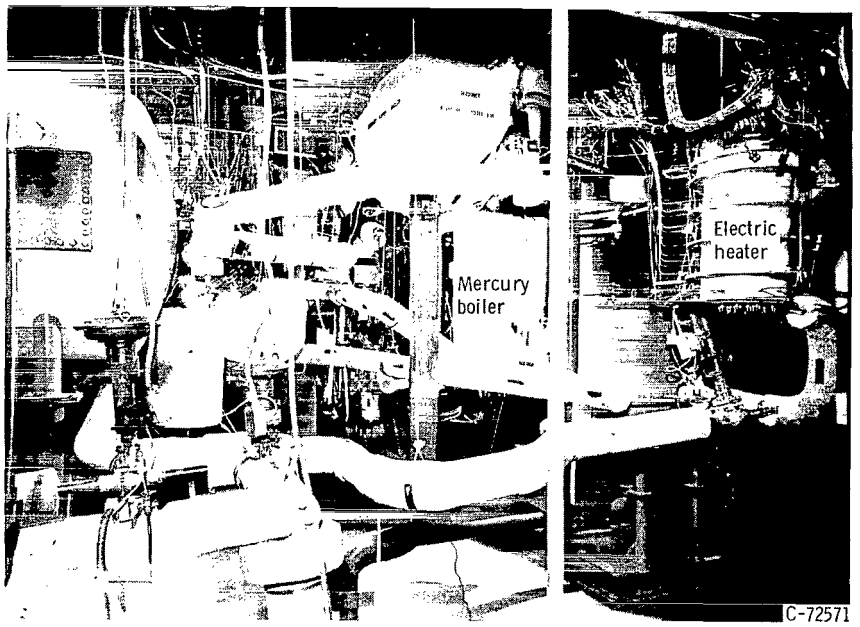

Figure 2. - Primary-loop area.

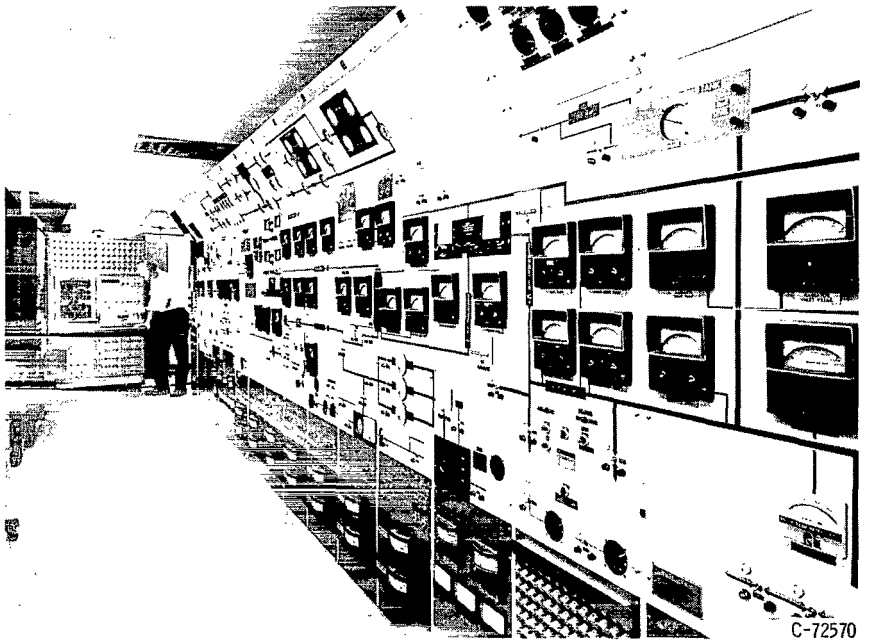

Figure 3. - Control room.

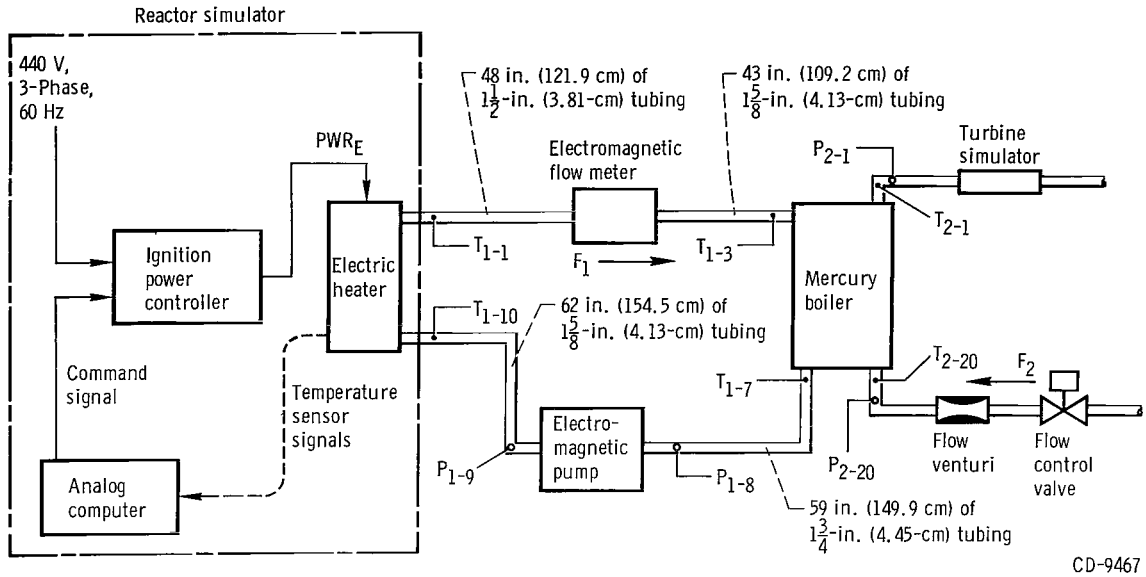

Figure 4. - Primary-loop configuration, electric heater power control and instrumentation identification.

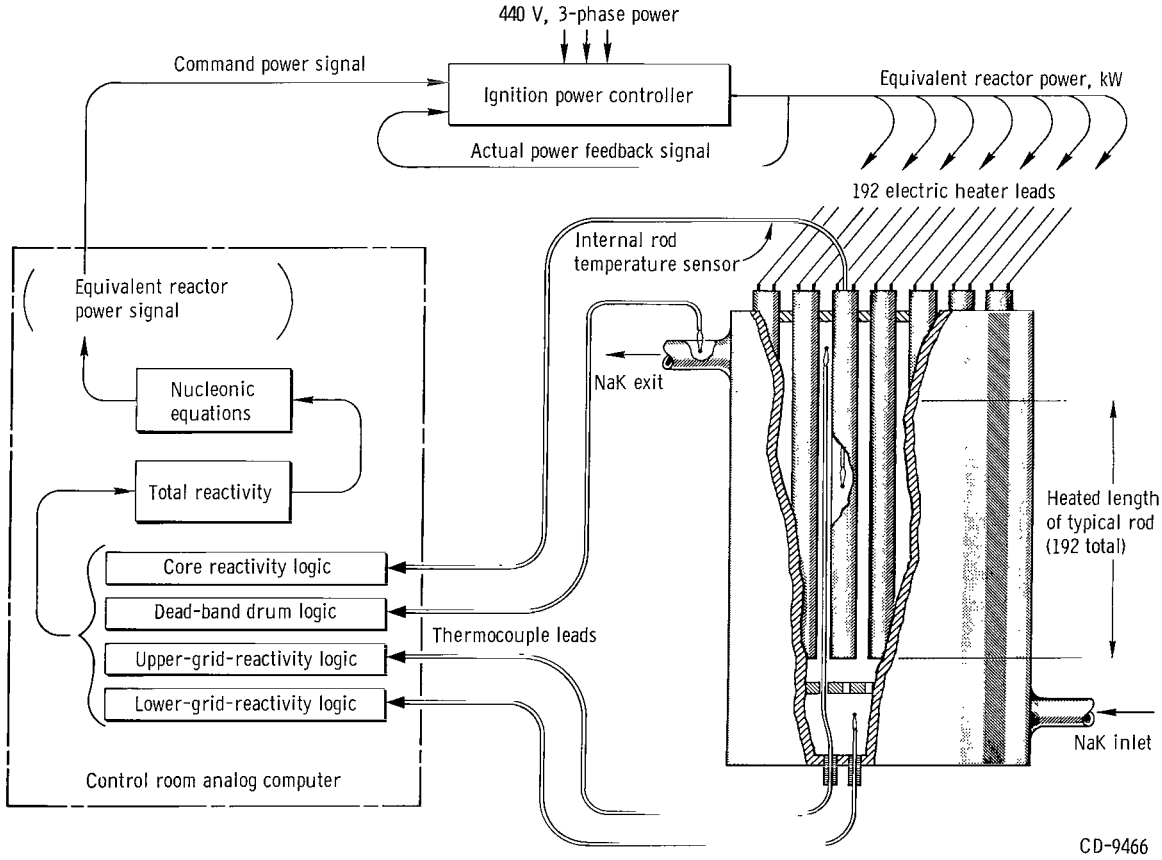

Figure 5. - Basic reactor-simulator system.

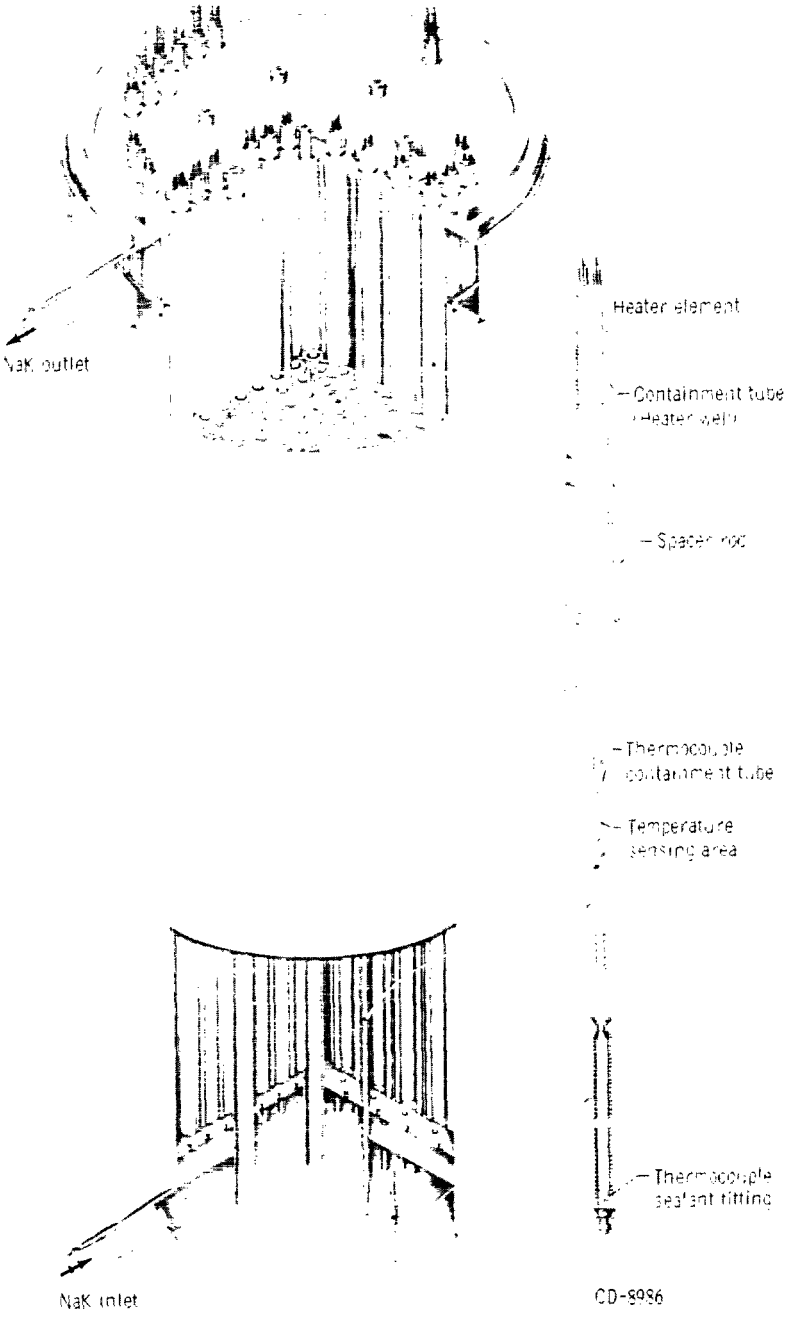

Figure 6. - Electric heater.

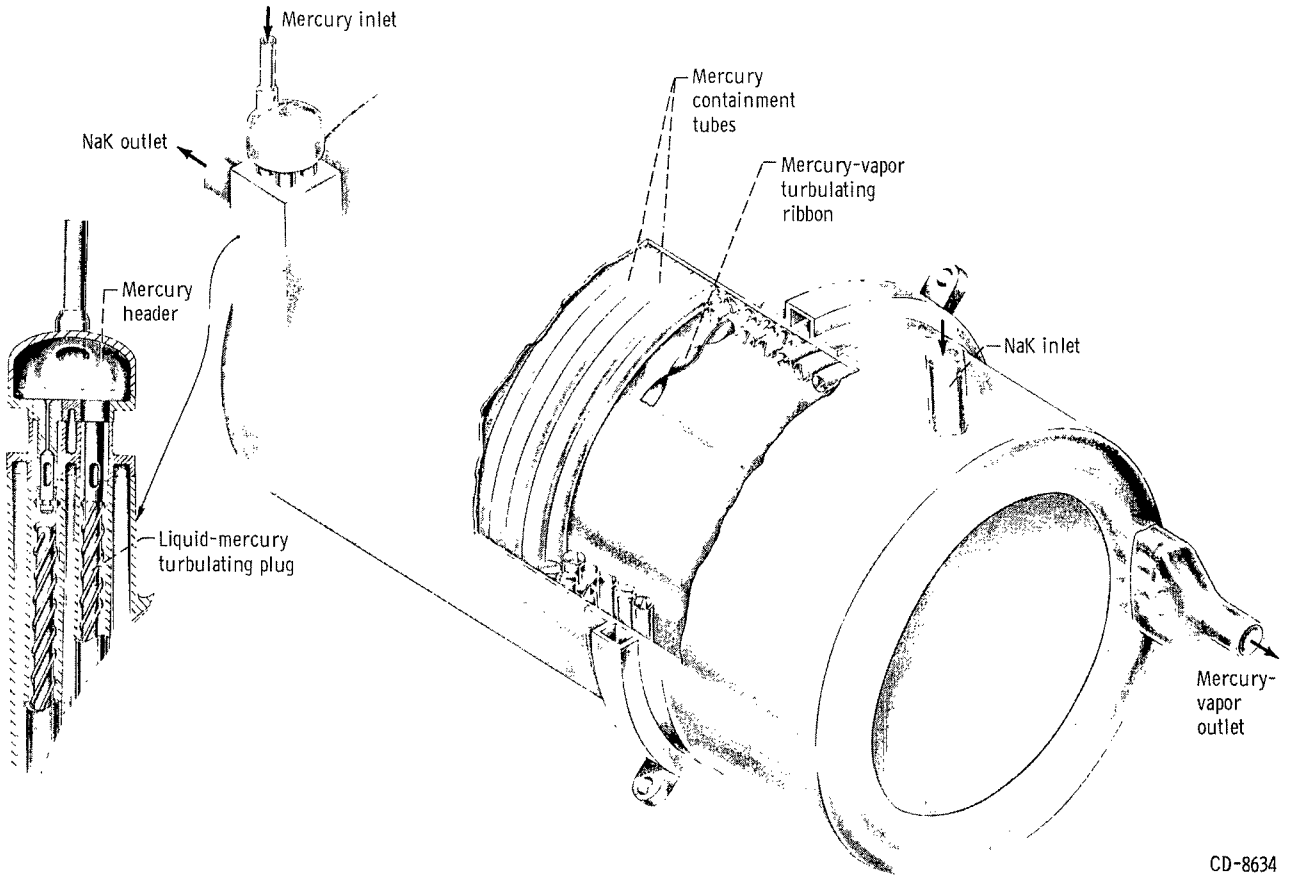

Figure 7. - Mercury boiler.

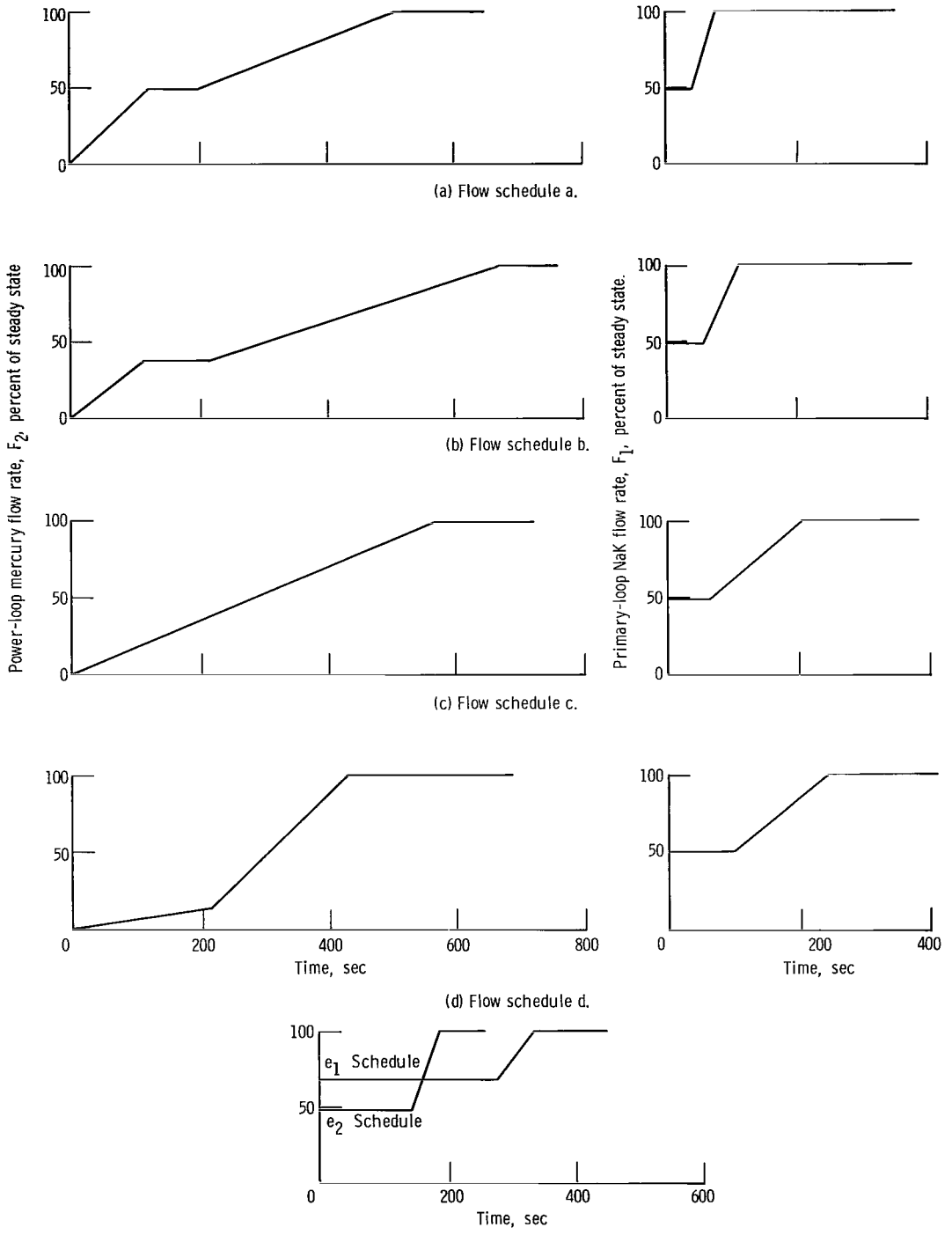

Figure 8. - Prescribed system flow schedules. Typically, 100 percent mercury flow, 9300 pounds per hour (4218 kg/hr); 100 percent primary NaK flow, 32 500 pounds per hour (14 742 kg/hr).

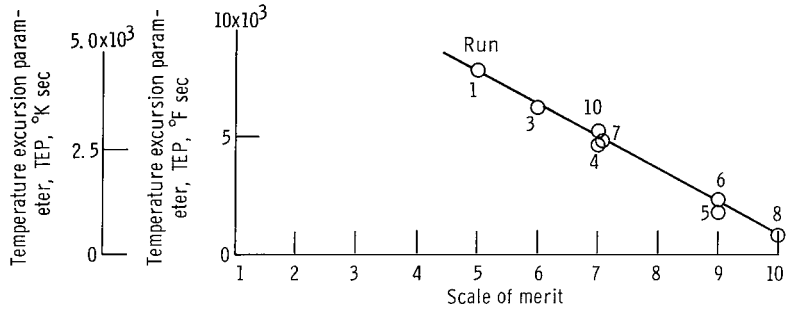

Figure 9. - Assignment of scale of merit based on value of reactor-simulator temperature excursion parameter.

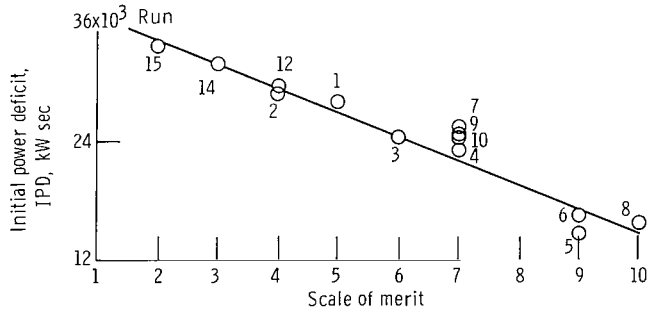

Figure 10. - Extrapolation of scale of merit utilizing initial power deficit so as to include runs which did not achieve steady-state operation.

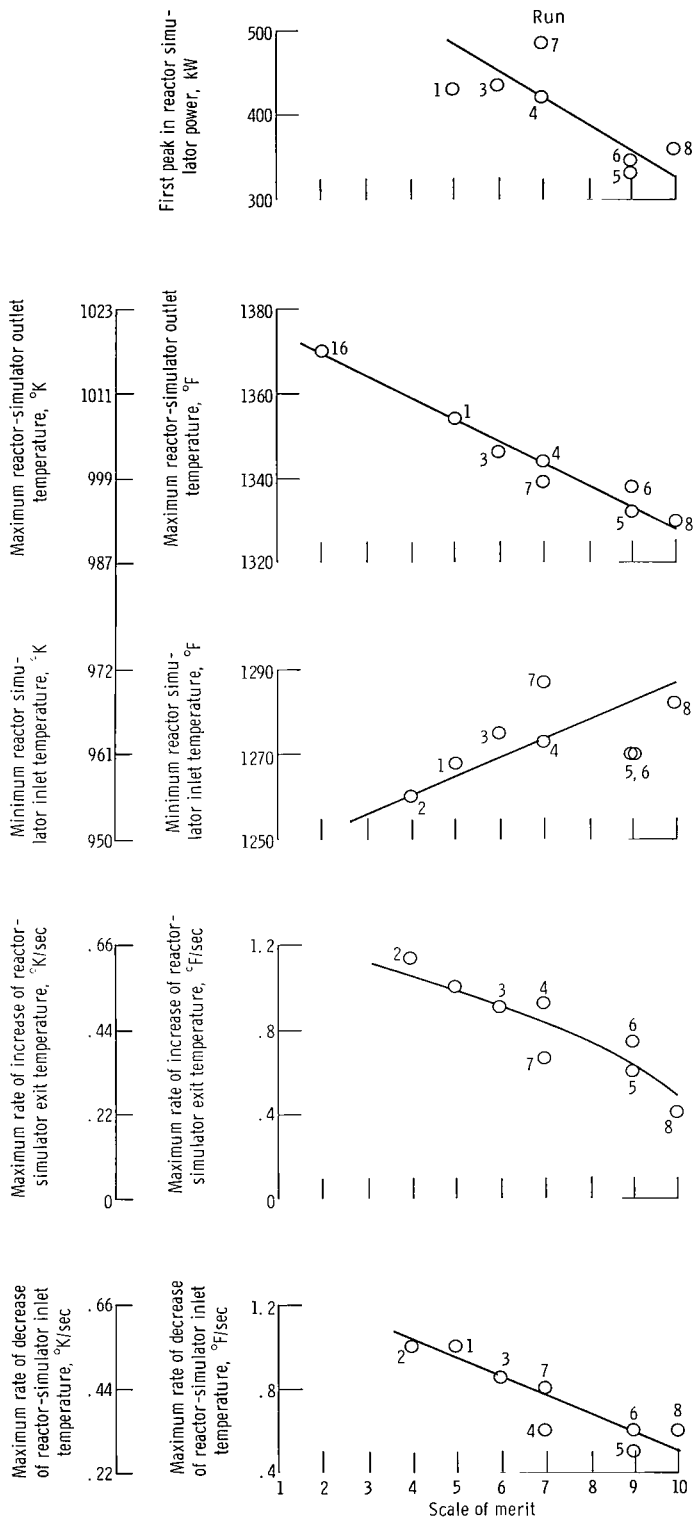

Figure 11. - Comparison of derived scale of merit with nuclear reactor constraints.

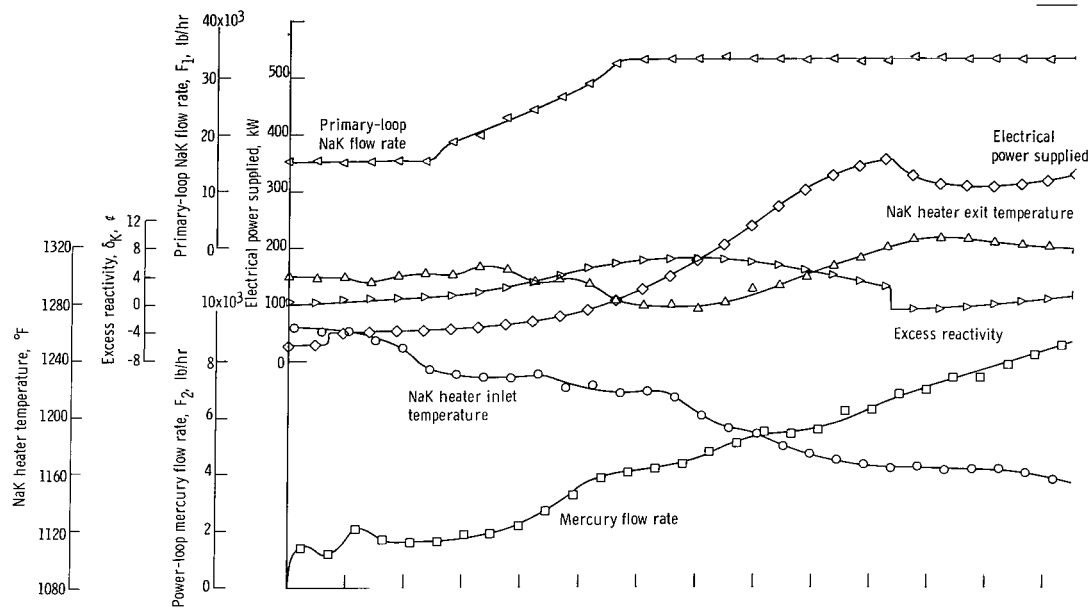

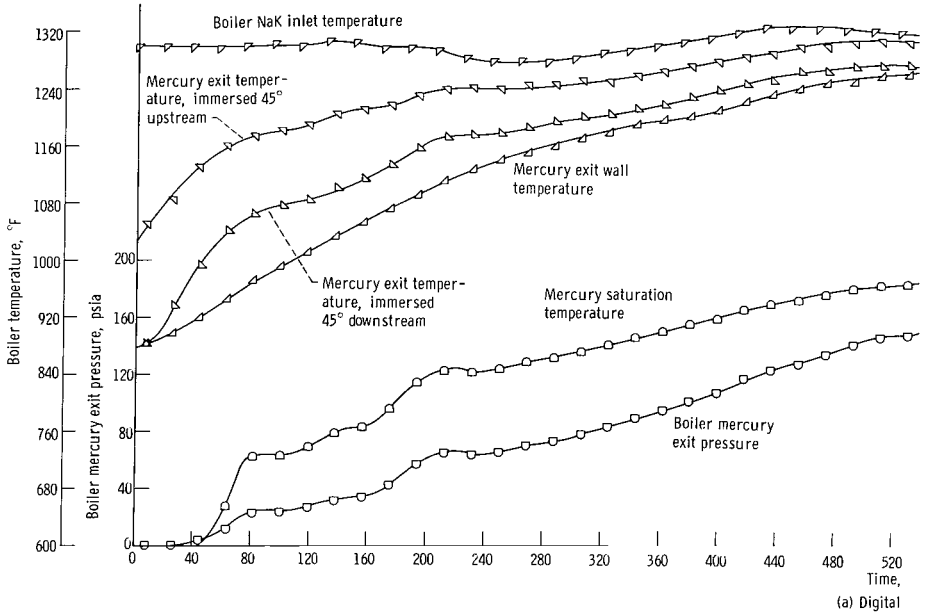

(a) Digital

Figure 12 - Results

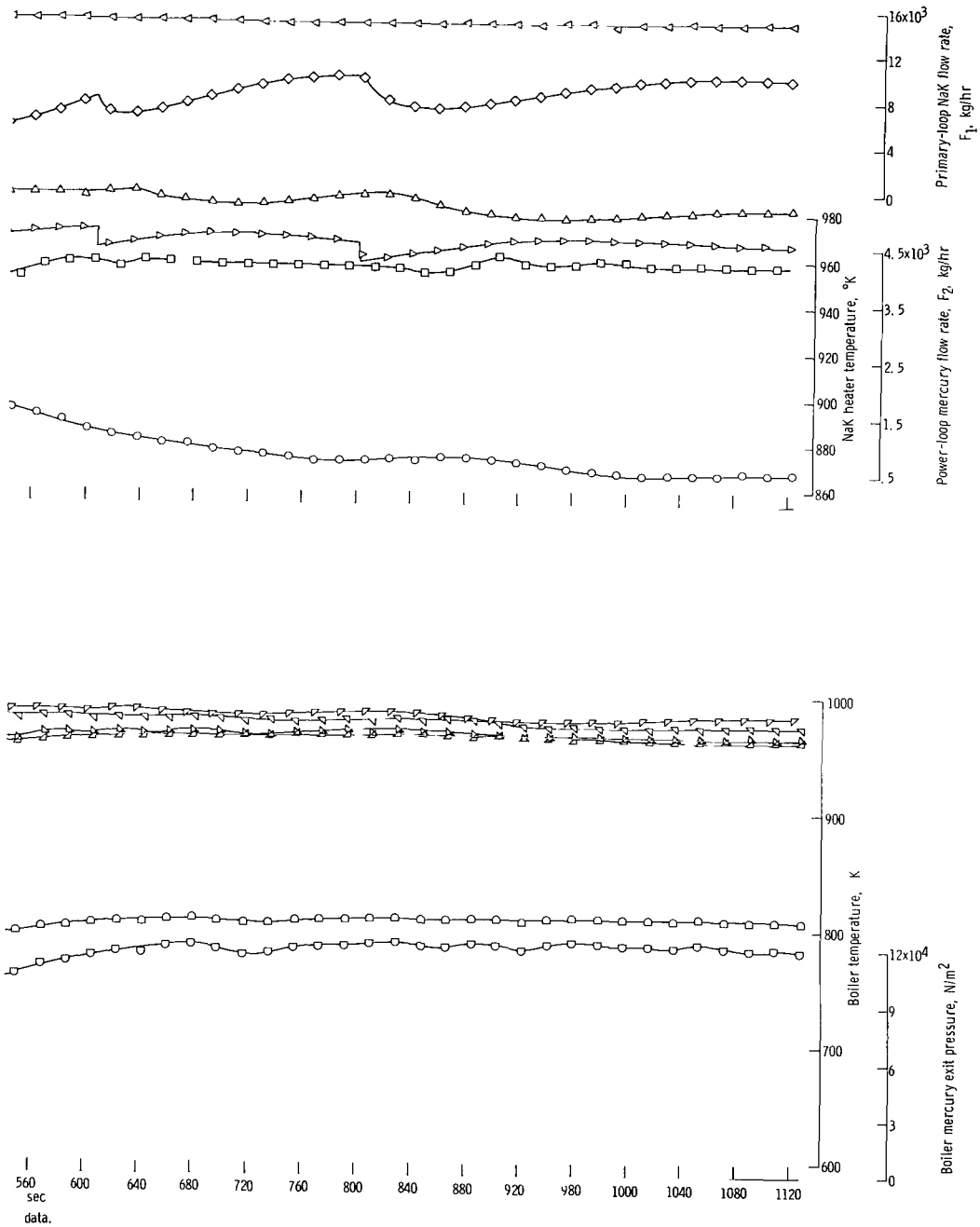

data.

for run 8.

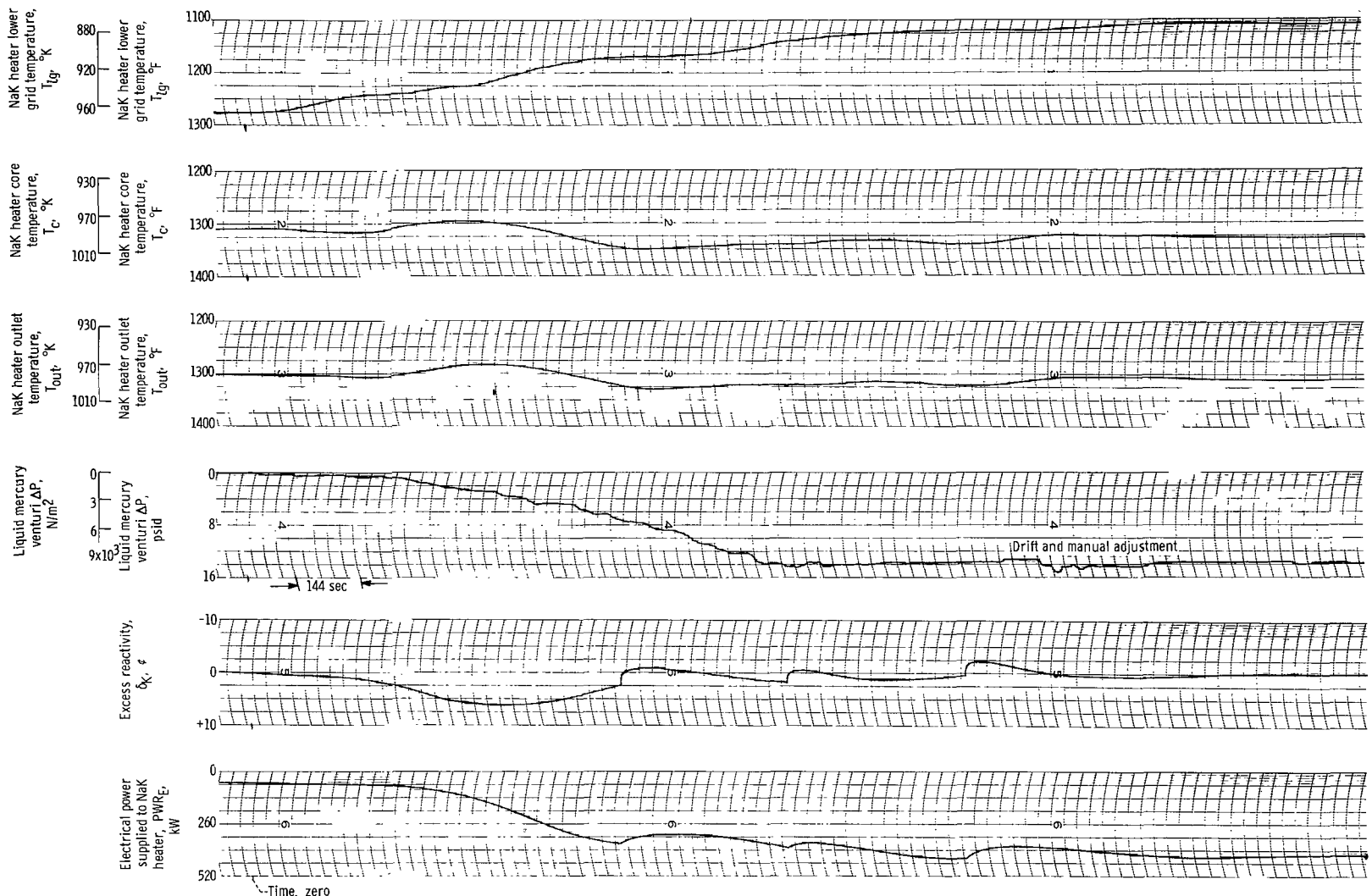

(b) Control-room recording.

Figure 12. - Concluded.

(a) Results of digital data.

Figure 13. - Results for run 11.

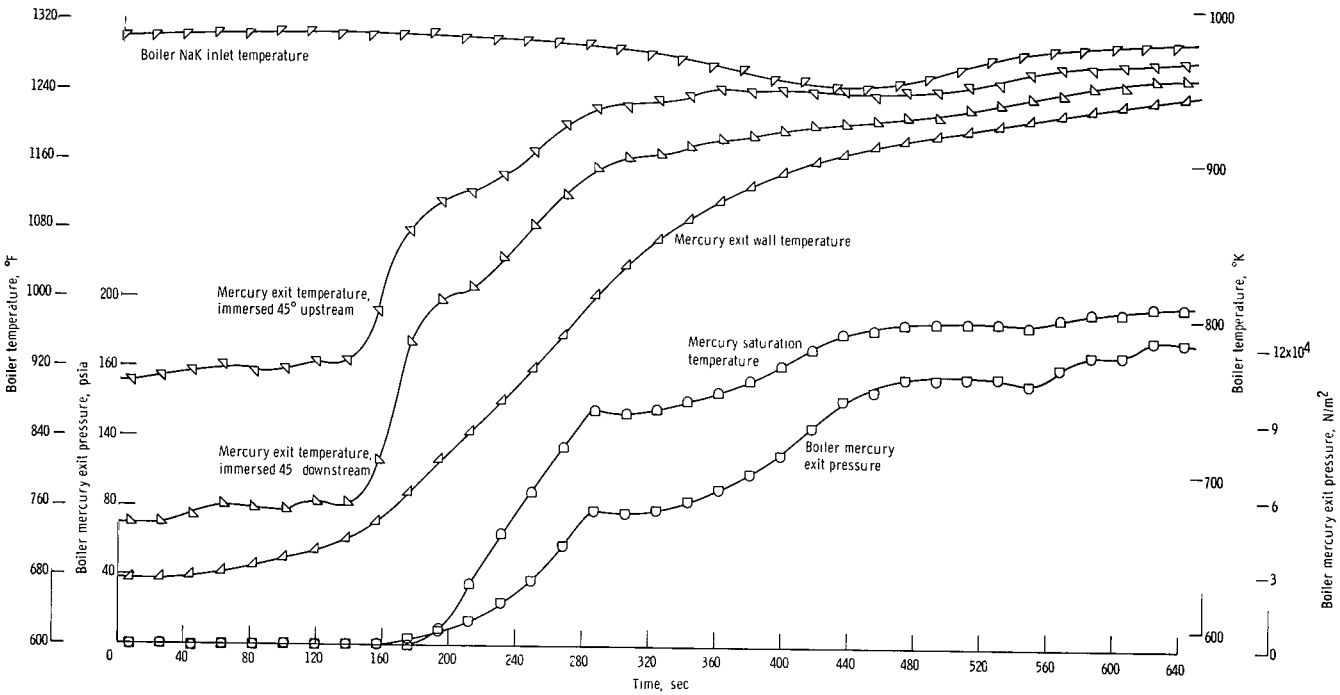

(a) Concluded.

Figure 13. - Continued.

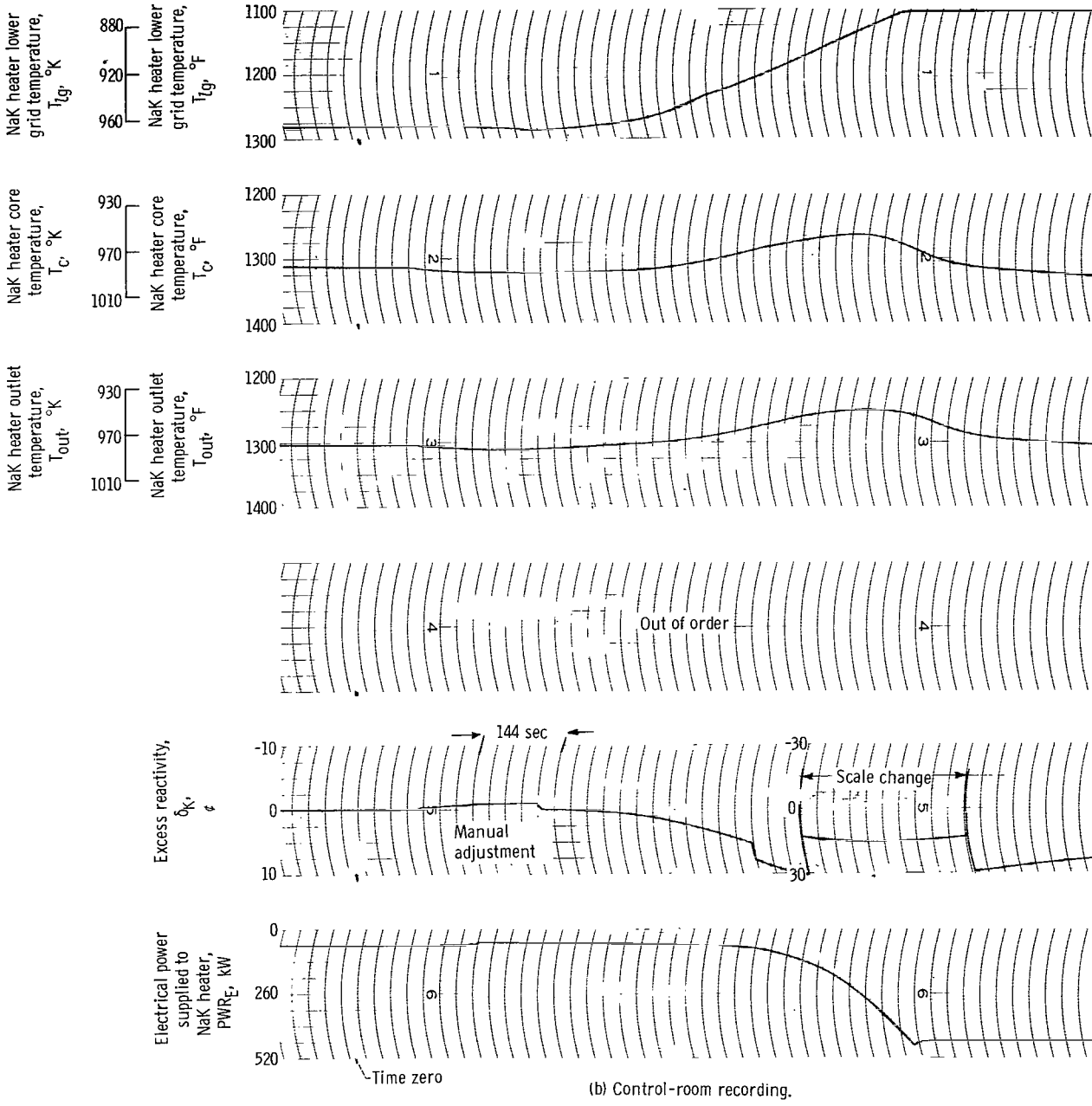

(b) Control-room recording.

Figure 13. - Concluded.

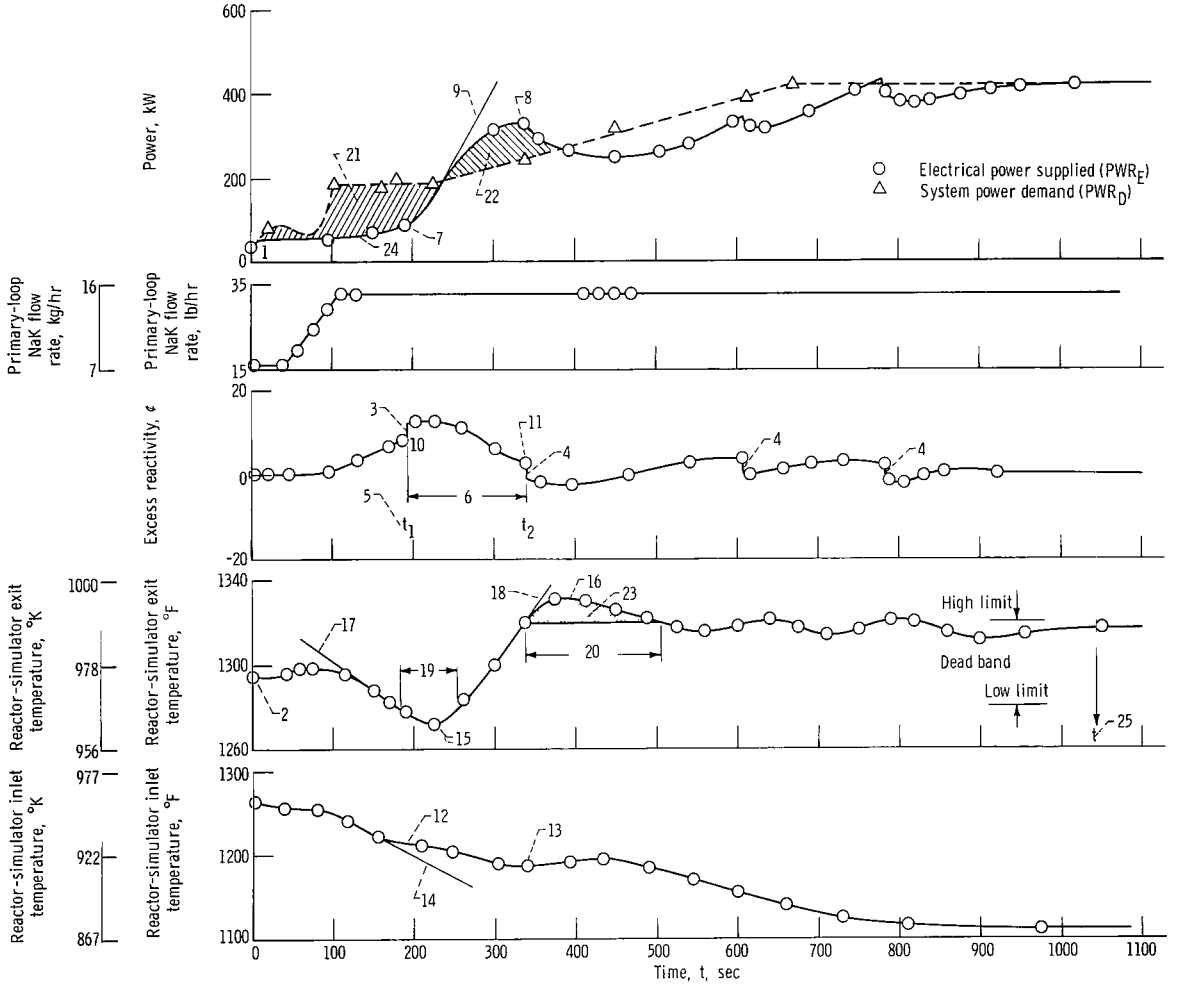

1 initial value of PWR_E
2 initial value of T_{1-1}
3 number of drum steps in
4 number of drum steps out
5 time of first drum step in
6 Δt between drum steps (in-out)
7 PWR_E at t_1
8 PWR_E at t_2
9 maximum $\Delta PWR_E/\Delta t$
10 δ_K at t_1
11 δ_K at t_2
12 T_{1-10} at t_1
13 T_{1-10} at t_2
14 maximum initial $\Delta T_{1-10}/\Delta t$
15 minimum T_{1-1}
16 maximum T_{1-1}
17 initial $\Delta T_{1-1}/\Delta t$ (drop)
18 maximum $\Delta T_{1-1}/\Delta T$ (rise)
19 Δt T_{1-1} outside lower dead band
20 Δt T_{1-1} initially outside upper dead band
21 energy deficit up to first crossover IPD
22 energy excess between first and second crossover SPE
23 temperature excursion parameter TEP
24 time required to inject 92 lb (41.73 kg) of mercury
25 total run time

Figure 14. - Typical startup illustrating key to generalized parameters (run 5). See table IV.

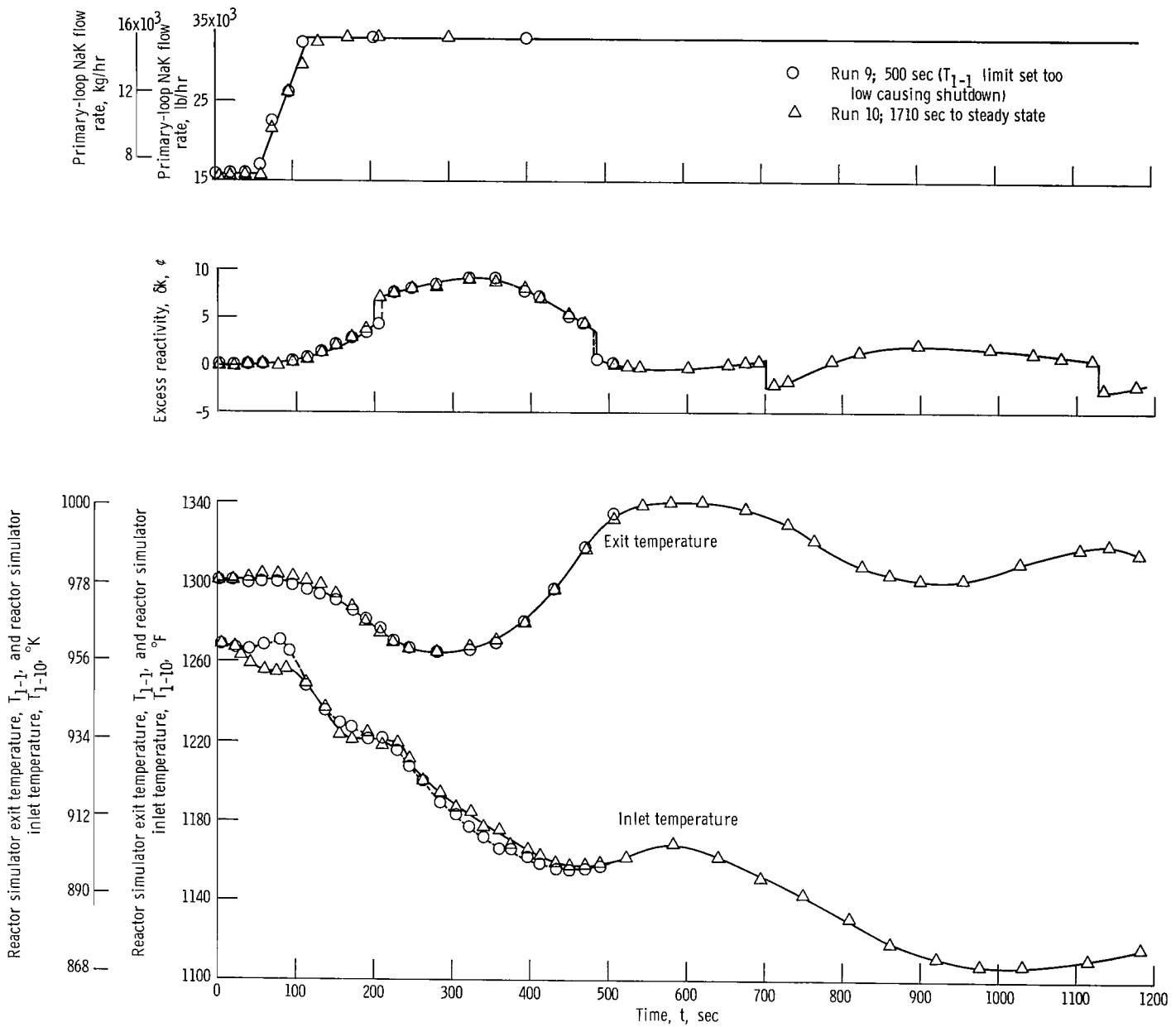

Figure 15. - Runs 9 and 10 illustrating system repeatability.

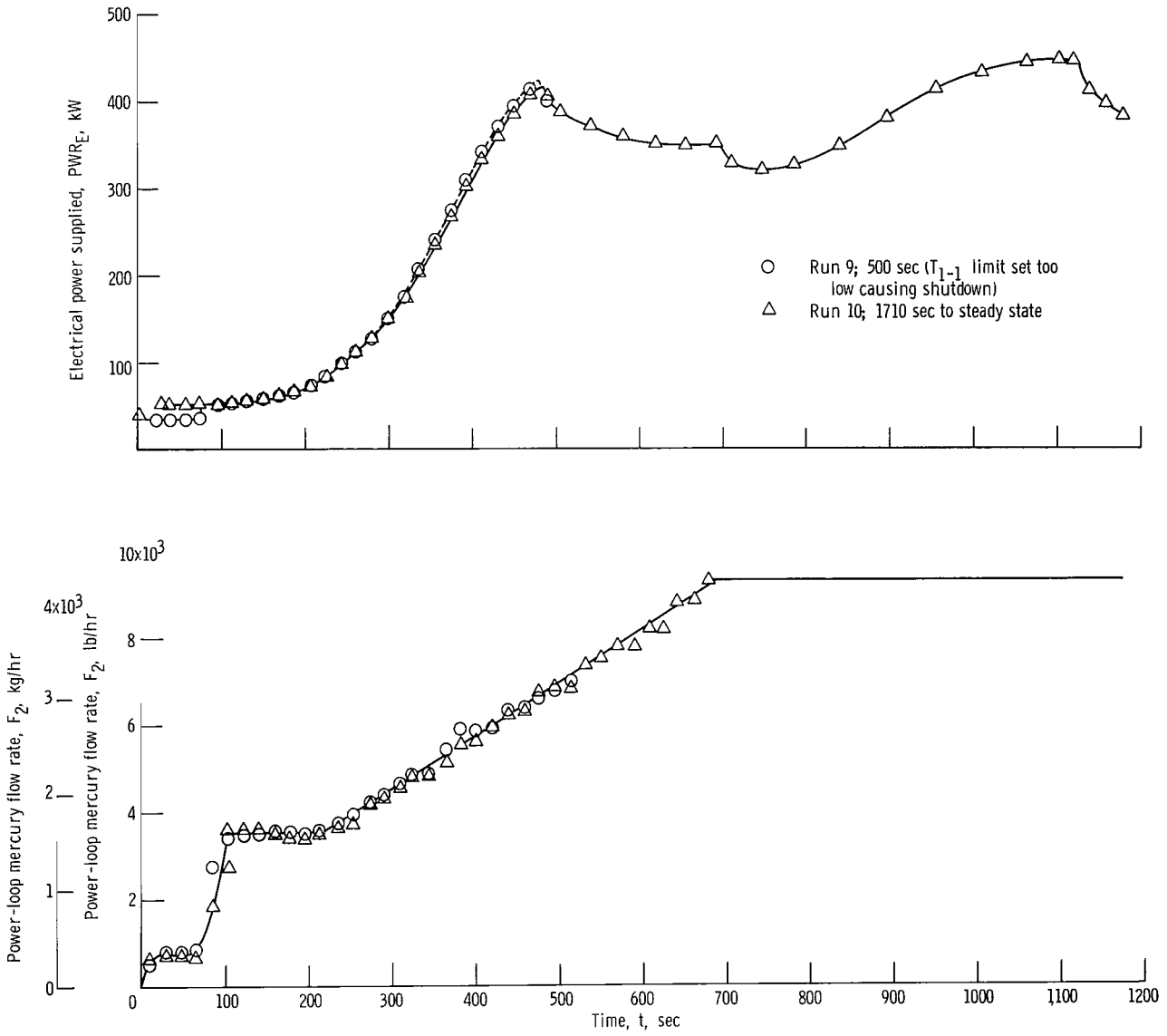

Figure 15. - Concluded.

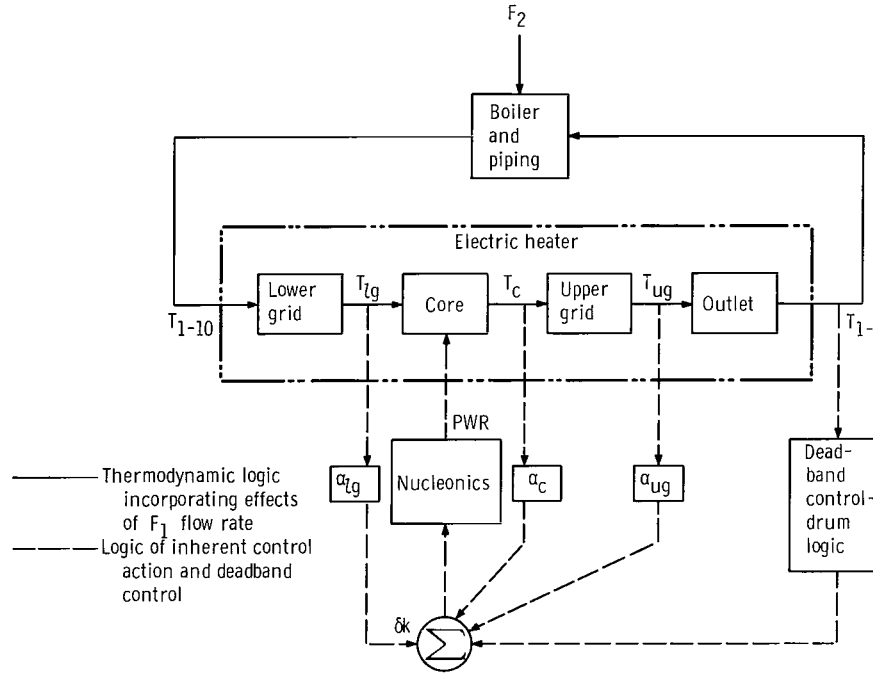

Figure 16. - Simplified block diagram of primary-loop logic.

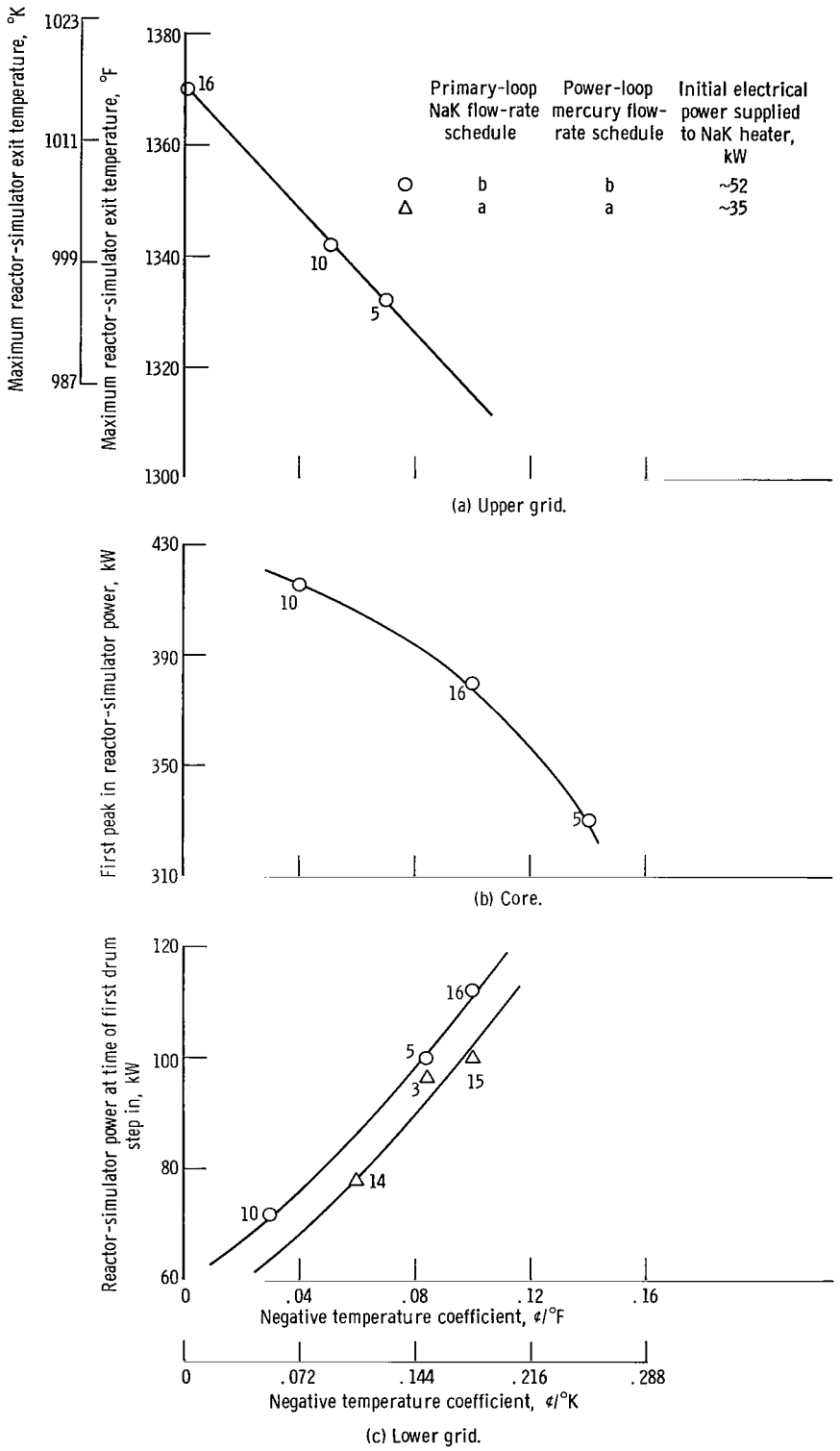

Figure 17. - Individual effects of reactor-simulator temperature coefficients for runs identical in all other respects.

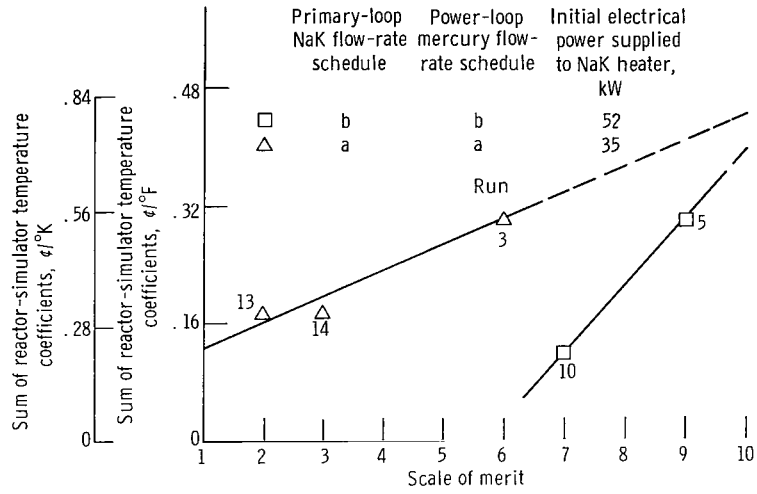

Figure 18. - Sum of the absolute values of the reactor-simulator temperature coefficients as function of scale of merit for runs similar in all other respects.

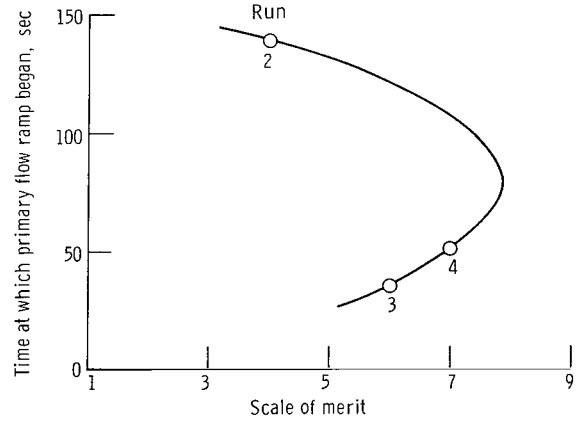

Figure 19. - Effect of primary loop flow transition time on startup merit for runs identical in all other respects.

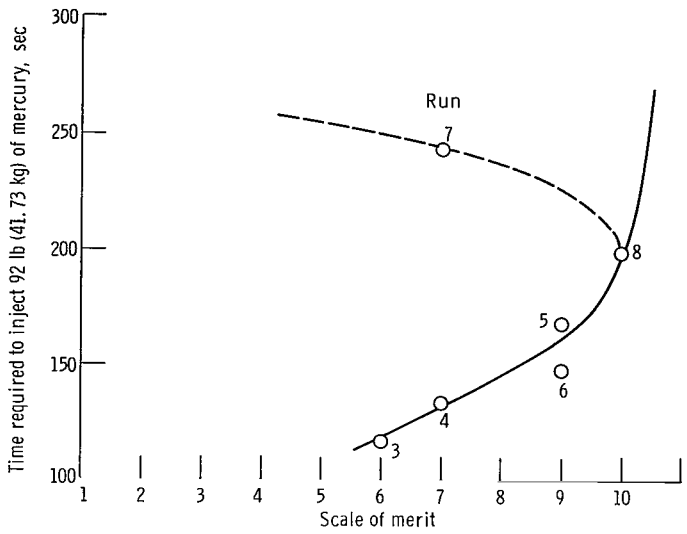

Figure 20. - Runs utilizing group D temperature coefficients illustrating effect of initial mercury flow schedule.

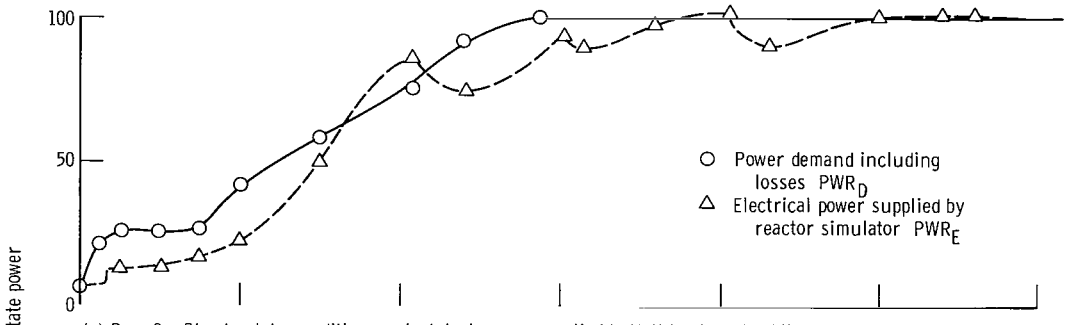

(a) Run 8. Steady-state conditions: electrical power supplied to NaK heater, 420 kilowatts; primary-loop NaK flow rate, 32 500 pounds per hour (14 742 kg/hr); power-loop mercury flow rate, 9300 pounds per hour (4218 kg/hr).

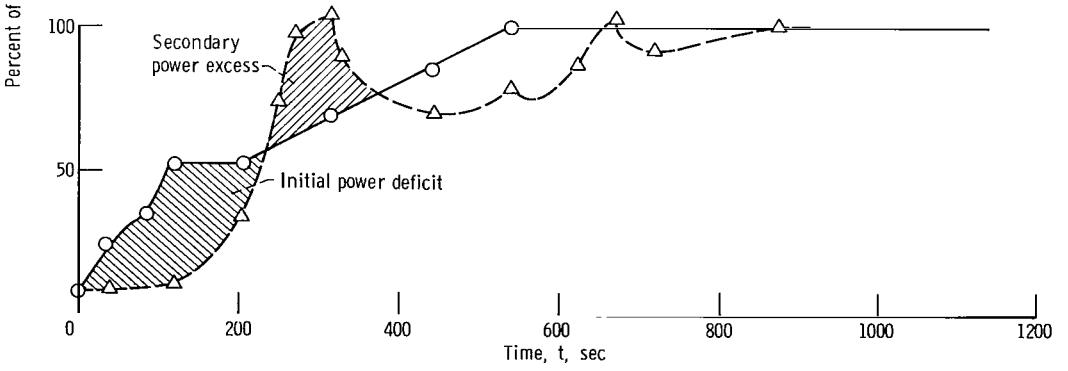

(b) Run 4. Steady-state conditions: electrical power supplied to NaK heater, 405 kilowatts; primary-loop NaK flow rate, 32 000 pounds per hour (14 515 kg/hr); power-loop mercury flow rate, 9000 pounds per hour (4082 kg/hr).

Figure 21. - Plot of electrical power supplied by reactor simulator and total system power demand for two startup transients.

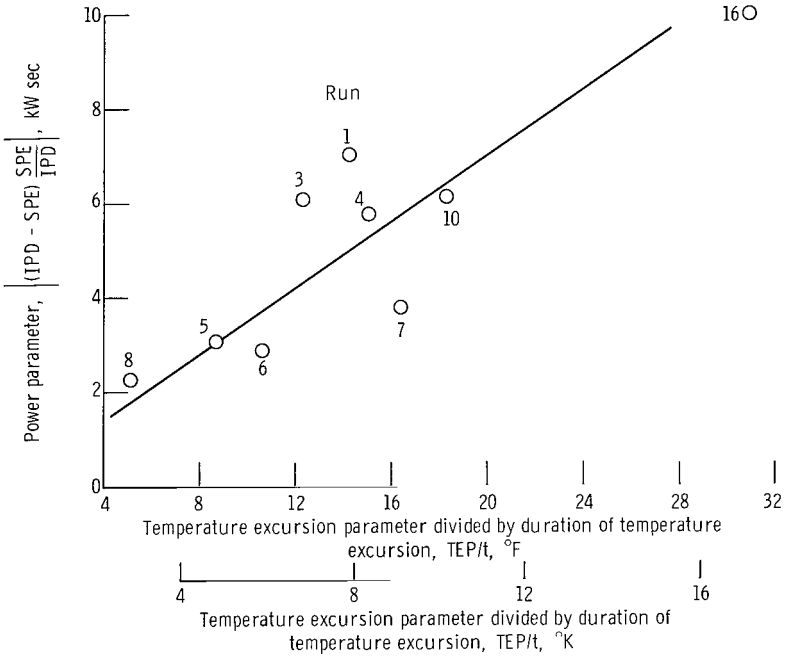

Figure 22. - Correlation between power parameter and average value of temperature excursion parameter.

NASA-Langley, 1968 — 3 E-4192

"The aeronautical and space activities of the United States shall be conducted so as to contribute . . . to the expansion of human knowledge of phenomena in the atmosphere and space. The Administration shall provide for the widest practicable and appropriate dissemination of information concerning its activities and the results thereof."

—NATIONAL AERONAUTICS AND SPACE ACT OF 1958

NASA SCIENTIFIC AND TECHNICAL PUBLICATIONS

TECHNICAL REPORTS: Scientific and technical information considered important, complete, and a lasting contribution to existing knowledge.

TECHNICAL NOTES: Information less broad in scope but nevertheless of importance as a contribution to existing knowledge.

TECHNICAL MEMORANDUMS: Information receiving limited distribution because of preliminary data, security classification, or other reasons.

CONTRACTOR REPORTS: Scientific and technical information generated under a NASA contract or grant and considered an important contribution to existing knowledge.

TECHNICAL TRANSLATIONS: Information published in a foreign language considered to merit NASA distribution in English.

SPECIAL PUBLICATIONS: Information derived from or of value to NASA activities. Publications include conference proceedings, monographs, data compilations, handbooks, sourcebooks, and special bibliographies.

TECHNOLOGY UTILIZATION PUBLICATIONS: Information on technology used by NASA that may be of particular interest in commercial and other non-aerospace applications. Publications include Tech Briefs, Technology Utilization Reports and Notes, and Technology Surveys.

Details on the availability of these publications may be obtained from:

SCIENTIFIC AND TECHNICAL INFORMATION DIVISION

NATIONAL AERONAUTICS AND SPACE ADMINISTRATION

Washington, D.C. 20546